

1 **Using Eddy Covariance Observations to Determine the Carbon**
2 **Sequestration Characteristics of Subalpine Forests in the**
3 **Qinghai-Tibet Plateau**

4 Niu Zhu^{1,2,4}, Jinniu Wang^{1,2}, Dongliang Luo³, Xufeng Wang³, Cheng Shen^{1,2}, Ning
5 Wu¹

6 1 Chengdu Institute of Biology, Chinese Academy of Science, Chengdu 610041,
7 China

8 2 Mangkang Ecological Monitoring Station, Tibet Ecological Security Barrier
9 Ecological Monitoring Network, Qamdo 854500, China

10 3 Northwest Institute of Eco-environmental Resources, Chinese Academy of
11 Sciences, Lanzhou 730000, China

12 4 College of Resources and Environmental Sciences, Gansu Agricultural University,
13 Lanzhou 730070, China

14 **Correspondence:** Jinniu Wang (wangjn@cib.ac.cn)

15 **Abstract:** The subalpine forests are one of the crucial components in the carbon cycling system in
16 the Qinghai-Tibet Plateau (QTP) in the context of climate change and ecosystem dynamics.~~The~~
17 ~~subalpine forests in the Qinghai-Tibet Plateau (QTP) act as carbon sinks in the context of climate~~
18 ~~change and ecosystem dynamics.~~ In this study, we investigated the carbon exchange dynamics for
19 a subalpine forest on the QTP using the eddy covariance method from November 2020 to October
20 2022. We first revealed the seasonal characteristics of carbon dynamics in the subalpine forest,
21 revealing the pattern of higher rates in summer and autumn and lower rates in winter and spring,
22 and found that autumn is the peak period for carbon sequestration in the subalpine forest.
23 Subsequently, we explored the climatic factors influencing the carbon sequestration function. The
24 PCA analysis show that photosynthetically active radiation (PAR) was major climatic factor
25 driving the net ecosystem exchange (NEE), significantly influencing forest and carbon absorption.
26 The spatial distribution of NEE was significantly positively correlated with temperature, while the
27 average annual precipitation shows a minor effect on NEE at the regional scale. At the annual
28 scale, the subalpine forest was a strong carbon sink, with an average NEE of -342 g C m^{-2} (from
29 November 2020 to October 2022). Despite the challenges caused by climate change, forests
30 remain a robust carbon sink, currently, they are the ecosystems with the highest carbon
31 sequestration capacity in the QTP, with an average annual CO_2 absorption rate of 368 gC m^{-2} . this
32 study provides essential insights for understanding the carbon cycling mechanism in plateau
33 ecosystems and the global carbon balance. We propose that, to positively influence global carbon
34 cycling and promote "carbon neutrality and peak carbon," strengthening the protection and
35 management of subalpine forests is crucial. Although our research has shown that these forest is
36 currently playing a role in continuous carbon absorption, there are significant data gaps on the
37 Qinghai-Tibetan Plateau. Therefore, it is essential to enhance continuous monitoring of forest
38 carbon absorption processes in the future.~~In this study, we investigated the carbon sequestration~~
39 ~~function using the *in-situ* observations from an eddy covariance system for the subalpine forests.~~
40 ~~With two-year contiguous observations, the factors driving the seasonal variations in carbon~~
41 ~~sequestration potential were quantified. We first revealed the seasonal characteristics of carbon~~
42 ~~dynamics in the subalpine forests during the growing and dormant seasons, respectively. The~~
43 ~~diurnal carbon exchange exhibited significant fluctuations, as high as $10.78 \mu\text{mol CO}_2 \text{ s}^{-1} \text{ m}^{-2}$~~

44 ~~(12:30, autumn). The period from summer to autumn was identified as the peak in carbon~~
45 ~~sequestration rate in the subalpine forests. Subsequently, we explored the climatic factors~~
46 ~~influencing the carbon sequestration function. Photosynthetically active radiation (PAR) was~~
47 ~~found to be a major climatic factor driving the net ecosystem exchange (NEE) within the same~~
48 ~~season, significantly influencing forest growth and carbon absorption. Increasing altitude~~
49 ~~negatively impacts carbon absorption at the regional scale and the rising annual temperature~~
50 ~~significantly enhances carbon uptake, while the average annual precipitation shows a minor effect~~
51 ~~on NEE. At the annual scale, the observations at the subalpine forests demonstrated a strong~~
52 ~~carbon sequestration capability, with an average NEE of 389.03 g C m⁻². Furthermore, we roughly~~
53 ~~assessed the carbon sequestration status of subalpine forests in the QTP. Despite challenges caused~~
54 ~~by climate change, these forests possess enormous carbon sequestration potential. Currently, they~~
55 ~~represent the most robust carbon sequestration ecosystem in the QTP. We conclude that enhancing~~
56 ~~the protection and management of subalpine forests under future climate change scenarios will~~
57 ~~positively impact global carbon cycling and contribute to climate change mitigation. Moreover,~~
58 ~~this study provides essential insights for understanding the carbon cycling mechanism in plateau~~
59 ~~ecosystems and global carbon balance.~~

60 **Keywords:** Subalpine forest; Qinghai-Tibet Plateau; The eddy covariance system; Three Parallel
61 Rivers Region; Carbon sinks

62 **1 Introduction**

63 Carbon dioxide (CO₂) is a prominent greenhouse gas, and its atmospheric concentration has
64 reached an unprecedented high level in recent years, in May 2021, a recorded peak of 419 parts
65 per million (ppm) was observed at the Mauna Loa Observatory in Hawaii (Stein, 2021).~~with a~~
66 ~~recorded peak of 419 parts per million (ppm). The global atmospheric CO₂ concentration is~~
67 ~~rapidly increasing at a rate of 2 to 3 ppm per year, compared to pre-industrial levels, the average~~
68 ~~global temperature has already risen by 1.1°C by 2019 (World Meteorological Organization,~~
69 ~~2019). Human activities have been the primary catalyst behind the significant surge in~~
70 ~~atmospheric CO₂ concentrations (Schweizer et al., 2020).~~~~Extensive research conducted by~~
71 ~~numerous scholars has consistently demonstrated that human activities have been the primary~~
72 ~~catalyst behind the significant surge in atmospheric CO₂ concentrations since the 18th century~~

73 ~~(Stein, 2021)~~. CO₂ and CH₄ collectively contribute approximately 70% to the global warming
74 potential among the six greenhouse gases specified in the Kyoto Protocol (Zhang et al., 2022). As
75 atmospheric CO₂ concentrations continue to rise, global climate warming is gradually intensifying.
76 Therefore, The Paris Agreement urges national governments to restrict the increase in global
77 average temperature to well below 2.0 °C above pre-industrial levels and to strive to limit it to
78 1.5 °C. The increasing atmospheric CO₂ levels will lead to irreversible ecological disasters. For
79 instance, the concentration of CO₂ in the atmosphere is projected to double within approximately
80 50 years if global consumption of fossil fuels continues to rise at the ~~current rate, the~~
81 ~~concentration of CO₂ in the atmosphere is projected to double within approximately 50 years. The~~
82 ~~rise in temperatures at 80°S latitude could result in the melting of glaciers, leading to a sea-level~~
83 ~~rise of 5 m (Mercer, 1978). By the year 2040, most countries are projected to experience at least~~
84 ~~one annual disaster with a 50% or higher probability (Fortunato et al., 2022)~~. Addressing the
85 greenhouse effect caused by carbon dioxide and reducing its impact is a crucial challenge facing
86 human society today. Reducing regional carbon emissions or per capita carbon emissions is
87 widely regarded as an effective approach to carbon reduction (Wang et al., 2023a). Nevertheless,
88 countries around the world have already begun to commit to carbon reduction and carbon
89 neutrality efforts. On September 22, 2020, during the 75th session of the United Nations General
90 Assembly, the Chinese government announced "double carbon" goals, which aim to achieve
91 carbon emission peaking by 2030 and carbon neutrality by 2060, in alignment with ecological
92 conservation and sustainable development objectives (Yu, 2022). It is predicted that China's
93 average forest carbon sequestration rate will reach 0.358 Pg C year⁻¹ (petagrams of carbon per
94 year) by 2060 (Cai et al., 2022). This significant rate of carbon sequestration is expected to have a
95 substantial impact on the environment and economy, providing negative feedback to global
96 warming (Pan et al., 2011).

97 ~~Currently, there are various methods available to accurately quantify the carbon sequestration~~
98 ~~potential of forests, each with its advantages and disadvantages. Forests cover approximately 30%~~
99 ~~of the earth's land surface and store around 90% of the terrestrial vegetation carbon (Le Quéré et~~
100 ~~al., 2018). However, currently, there is no method available to accurately quantify the carbon~~
101 ~~sequestration potential of forests.~~ Quantitative estimation of carbon sequestration potential still

102 requires scientists to establish more *in-situ* sites and generate comprehensive datasets to assess a
103 wide range of areas. Initially, individuals' biomass measurements were used to estimate forest
104 carbon sequestration capacity (Ebermayer, 1876). However, this method was time-consuming,
105 labor-intensive, and prone to inaccuracies due to the omission of various variables during the
106 calculation process. The development of modeling techniques allowed for the use of simulation
107 methods - forest management models and land ecosystem-climate interaction models, such as the
108 Ecological Assimilation of Land and Climate Observation (EALCO), have been widely applied in
109 this regard (Landsberg and Waring, 1997; Wang et al., 2001). Currently, remote sensing
110 monitoring and the eddy covariance method are widely used. Remote sensing techniques can be
111 used to extract vegetation parameters (such as NDVI) from multispectral bands and estimate the
112 carbon sequestration of entire forests through regression analysis (Laurin et al., 2014). The eddy
113 covariance (EC) method, allowing continuous, long-term carbon flux calculation, provides
114 fundamental data for model establishment and calibration. It is widely applied across ecosystems,
115 including urban areas, farmlands, grasslands, forests, and water bodies (Konopka et al., 2021;
116 Vote et al., 2015; Du et al., 2022a; Kondo et al., 2017; Li et al., 2022).~~The theoretical foundation
117 of the eddy covariance method was initially proposed by Swinbank et al., (Swinbank, 1951). It
118 started to be applied in carbon flux studies of forest ecosystems in the 1980s (Anderson et al.,
119 1984). Nowadays, this method not only accurately measures the carbon exchange between forests
120 and the atmosphere but also integrates other instruments to measure meteorological variables such
121 as light intensity and temperature. It allows for long-term and continuous calculation of carbon
122 flux between forests and the atmosphere. Additionally, it provides fundamental data for
123 establishing and calibrating other models. The eddy covariance method has been widely applied in
124 various ecosystems, including urban areas (Konopka et al., 2021), farmlands (Vote et al., 2015),
125 grasslands (Du et al., 2022a), forests (Kondo et al., 2017), and water bodies (Li et al., 2022).~~

126 The forest ecosystem's Net ecosystem exchange (NEE) of carbon dioxide is influenced by
127 multiple environmental factors~~Net Ecosystem Exchange (NEE) of carbon dioxide is a
128 fundamental parameter in the biogeochemical feedback of the climate system (Graf et al., 2013).
129 The carbon flux in forest ecosystems is influenced by multiple environmental factors.~~ Previous
130 studies have shown that NEE is significantly influenced by air temperature (AT),

131 photosynthetically active radiation (PAR), vapor pressure deficit (VPD), relative humidity (RH),
132 and soil temperature (ST) (Liu et al., 2022). For instance, temperature variables, especially annual
133 or seasonal average temperature variations, serve as the optimal single predictor for carbon flux,
134 explaining variations in carbon flux between 19% and 71% (Banbury Morgan et al., 2021).
135 Photosynthetically active radiation not only influences the absorption of carbon dioxide by the
136 forest canopy but also affects the utilization of carbohydrates by roots due to its association with
137 canopy processes and soil respiration (Baumgartner et al., 2020). Furthermore, research suggests
138 that the NEE is influenced by biotic factors such as NDVI (Normalized Difference Vegetation
139 Index) and LAI (Leaf Area Index) (Tang et al., 2022). Given the projected future global warming
140 trends, the role of forests as a vast carbon reservoir becomes highly significant and worthy of
141 attention. The Qinghai-Tibet Plateau (QTP) is the highest and largest plateau in the world, with an
142 extensive area of alpine forests covering approximately 2.3×10^5 km². These forests hold
143 tremendous economic and ecological benefits. The southeastern region of the QTP boasts one of
144 the world's highest-altitude alpine forest ecosystems. Research indicates that the alpine forest
145 ecosystem in this area has a remarkable capacity to consume methane, reaching up to 5.06 kg ha⁻¹
146 yr⁻¹, and playing a significant role in mitigating the impact of greenhouse gases (Qu et al., 2023).
147 Since the 1960s, the QTP has experienced a faster warming rate than lowland areas. It is projected
148 that this phenomenon will be intensified by the end of the 21st century (Li et al., 2019). Currently,
149 the QTP is considered a weak carbon sink at the overall level, but the carbon source-sink
150 dynamics vary among different ecosystems (Chen et al., 2022). For instance, most lakes in the
151 QTP are currently characterized by supersaturated CO₂ levels (Cole et al., 1994). Mu et al. (2023)
152 found that the thermokarst lakes serve as significant carbon sources through carbon flux
153 measurements in 163 thermokarst lakes during the summer and autumn seasons. Wang et al. (2021)
154 discovered that these ecosystems act as sinks for carbon dioxide by comparing carbon fluxes in
155 ten high-mountain ecosystems with different grassland types.~~Wang et al. (2021), discovered that~~
156 ~~these ecosystems act as sinks for carbon dioxide in their study comparing carbon fluxes in ten~~
157 ~~high-mountain ecosystems with different grassland types.~~ The alpine meadows in the eastern QTP
158 were identified as strong carbon sinks, with the highest annual average NEE recorded at -284 g C
159 m⁻². Forest ecosystems play a crucial role in the south-eastern edge of the QTP, providing

160 important support for climate regulation and forestry-based economic activities. Moreover, recent
161 predictive studies suggest that under both current and future climate scenarios, the forested area in
162 this region is expected to expand further, with coniferous forests continuing to grow into higher
163 altitudes (Liu et al., 2021). Due to the extensive presence of permafrost in the QTP, forest net
164 primary productivity exhibits a most pronounced response to surface temperatures in the
165 continuous permafrost zone over multiple years. Therefore, the changes in permafrost in the QTP
166 should not be overlooked, as they also have a significant impact on carbon absorption by forests
167 (Mao et al., 2015). However, the QTP is a vast region with a widespread distribution of
168 high-altitude and subalpine forests. Researchers need to conduct long-term monitoring to
169 understand how these forests will respond to climate change. Furthermore, there is a significant
170 data gap concerning the monitoring of carbon exchange capacity in the forests of the QTP,
171 indicating the need for further data collection efforts. Based on this, we have established a carbon
172 flux monitoring site in the subalpine ecosystem of the Three Parallel Rivers Region, which is
173 located on the south-eastern edge of the QTP and lies in the transitional zone between the QTP
174 and the Yunnan-Kweichow Plateau and is renowned as a global hotspot for biodiversity (Wang et
175 al., 2022). Our research objectives are as follows:

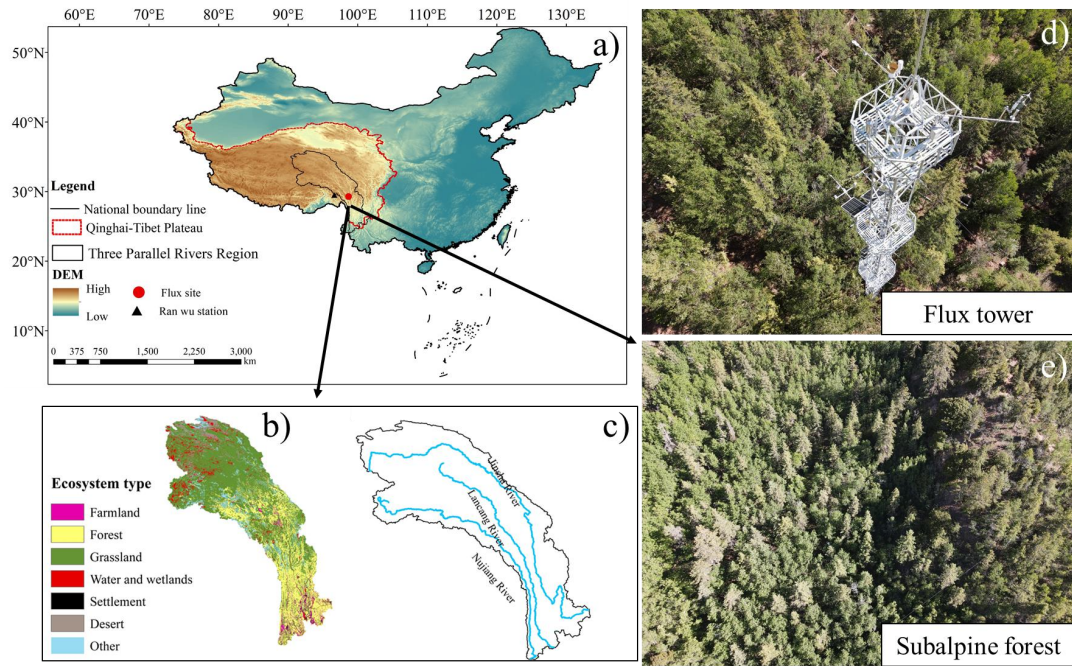
- 176 1) Determine whether the subalpine forests in the Three Parallel Rivers Region act as a carbon
177 sink or source, and quantify the annual uptake or release of carbon dioxide;
- 178 2) Investigate the main environmental factors influencing the carbon exchange process in the
179 subalpine forests and identify the factors with the greatest impact;
- 180 3) Since the carbon sink potential of forest ecosystems in the QTP is currently unknown, we
181 evaluated the carbon exchange capacity of subalpine forests by comparing existing data with
182 other ecosystems in the QTP.~~Assess the carbon exchange capacity of the subalpine forests in~~
183 ~~comparison to other ecosystems of the QTP.~~

184 This study will provide a data foundation and background support for accurately estimating
185 the carbon balance of forests in high-altitude areas and for model simulations in the future.

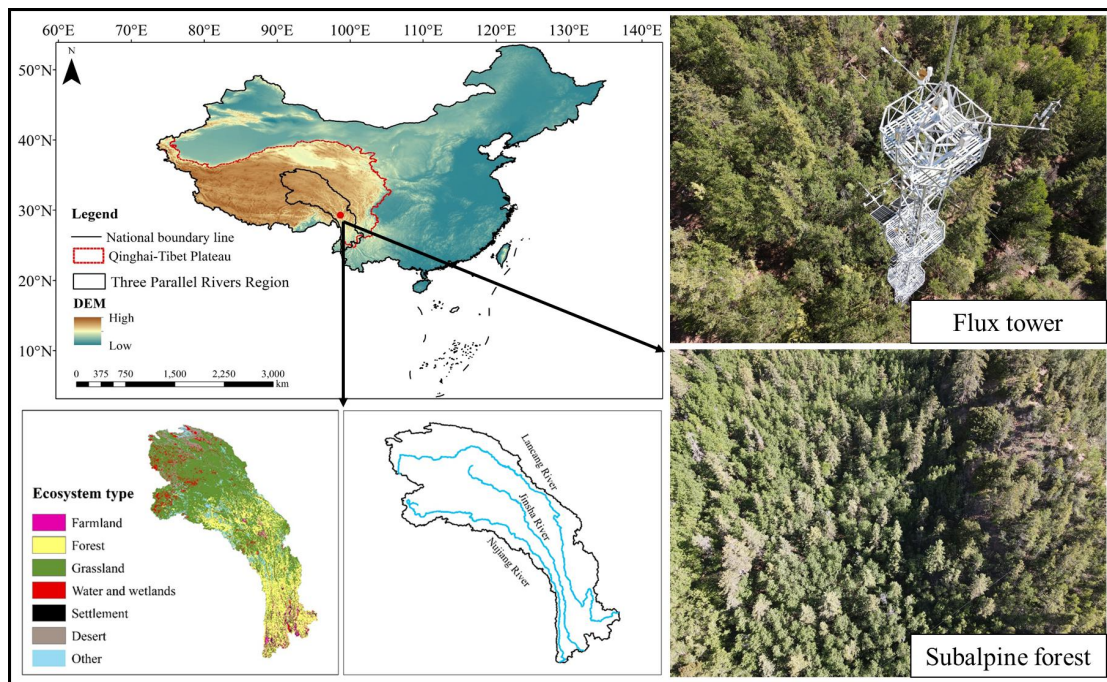
186 **2 Materials and Methods**

187 2.1 Overview of the study site

188 The study site is located in the Hongla Mountain Yunnan Snub-nosed Monkey National
189 Nature Reserve in Mangkang County, Tibet, China (29.28633°N, 98.69096°E), the core area of
190 the Three Parallel Rivers (Nujiang River, Lancang River, and Jinsha River) Region. The elevation
191 of the study site is 3755 m. The observation period was from November 2020 to October 2022.
192 The study area experiences large diurnal temperature variations and dry conditions in winter,
193 while the summers are warm and humid. ~~The climate of the region is characterized as a typical~~
194 ~~mountainous climate.~~ The average daily sunshine duration exceeds 10 h, with an annual average
195 temperature of 5 °C and an average annual precipitation of around 600 mm (Niu et al., 2023). The
196 main tree species in the area include *Picea likiangensis* var. *rubescens*, *Abies squamata*, *Sabina*
197 *tibetica* Kom, and *Abies ernestii*. They are accompanied by the growth of some *Quercus*
198 *aquifolioides*, *Rhododendron lapponicum*, and *Potentilla fruticosa* shrubs. The average height of
199 the trees is below 30 meters, and the forest is in a relatively active growth phase, reaching the state
200 of a mature forest. The vegetation coverage ranges from 70% to 80%.~~The vegetation coverage~~
201 ~~ranges from 70% to 80%, indicating rich vegetation resources.~~ The dominant soil type is
202 yellow-brown soil. The mountainous terrain contributes to distinct vertical climate characteristics
203 and significant variations in water and heat conditions. Characterized by numerous dry and hot
204 river valleys and widespread distribution of canyons, the climate in the study area exhibits a clear
205 impact from the southwest and southeast monsoons. The varying elevations give rise to diverse
206 ecosystems, transitioning from alpine forests to mountain shrubs, and above 4000 meters, high
207 alpine grasslands and meadows, forming a noticeable vegetation transition zone. The mountainous
208 topography results in evident vertical climate features and significant fluctuations in water and
209 heat conditions, with precipitation showing a pronouncedly uneven distribution throughout the
210 region (Zemin et al., 2023).~~The study site is located in the core area of the Three Parallel Rivers~~
211 ~~(Nujiang River, Lancang River, and Jinsha River) Region. The area exhibits a complex and~~
212 ~~diverse climatic environment influenced by the southwest and southeast monsoon. The~~
213 ~~mountainous terrain contributes to distinct vertical climate characteristics and significant~~
214 ~~variations in water and heat conditions. The region is characterized by numerous dry and hot river~~
215 ~~valleys and widespread distribution of canyons.~~



216



217

218 Figure 1. location of the flux site (a). Ecosystem types (b) and main rivers (c) in Three Parallel
 219 Rivers Region. Flux tower (d) and forest top view (e). (The national boundary range in the figure
 220 was retrieved from the <http://bzdt.ch.mnr.gov.cn>, elevation data, and ecosystem type from
 221 www.gscloud.cn.)Figure 1 Overview of the study area (The national boundary range in the figure
 222 comes from the <http://bzdt.ch.mnr.gov.cn>, elevation data from www.gscloud.cn.)

223 2.2 Eddy covariance system

224 ~~The flux data in this study were collected from a 35 m-high tower located at the study~~
225 ~~site. The flux data in this study were collected from a 35 m-high tower located at the study site.~~ At
226 the top of the tower, a 3-D wind velocity (Wind Master, Gill, UK) and an open-path infrared
227 CO₂/H₂O analyzer (LI-7500DS, Li-Cor, USA) were installed to measure CO₂ flux. ~~The~~
228 ~~instruments had a measurement frequency of 10 Hz. The instruments had a response frequency of~~
229 ~~10 Hz.~~ Additionally, micro-meteorological sensors were placed at different heights on the tower,
230 ~~including sensors at 15 m for observing air temperature and humidity (HMP155A, Vaisala,~~
231 ~~Finland), sensors at -5 cm for soil temperature (TEROS11, LI-Cor, USA), and sensors at 35 m for~~
232 ~~photosynthetically active radiation (LI-190R, LI-Cor, USA), including sensors for observing air~~
233 ~~temperature and humidity (HMP155A, Vaisala, Finland), soil temperature (TEROS11, LI-Cor,~~
234 ~~USA), and photosynthetically active radiation (LI-190R, LI-Cor, USA),~~ among other
235 environmental variables. All data were recorded at 30-m intervals and stored in a SmartFlux 3 data
236 logger (Li-Cor, USA) for future download.

237 2.3 Data processing and quality control

238 ~~When considering only the turbulent transport of matter and energy in the vertical direction,~~
239 ~~the carbon dioxide flux (F_c) can be represented by the following equation (Yu and Sun, 2006;~~
240 ~~Monteith et al., 1994): Turbulent transport is the primary form of gas exchange between the~~
241 ~~near surface and the atmosphere. In the case of a homogeneous and flat underlying surface,~~
242 ~~considering only the turbulent transport of substances in the vertical direction, the CO₂ flux F_c~~
243 ~~(μmol m⁻² s⁻¹ or mg m⁻² s⁻¹) within the region can be calculated using the following:~~

$$244 \quad F_c = \overline{W' CO_2'} \quad (1)$$

245 ~~Where W' is the vertical component of 3-D wind speed fluctuations (m s⁻¹), and CO₂' represents~~
246 ~~the fluctuations in measured CO₂ mole concentration. A positive F_c indicates carbon emissions,~~
247 ~~while a negative value represents carbon uptake. Where W' represents the vertical component of~~
248 ~~3-D wind speed fluctuations (m/s), CO₂' represents the fluctuations in measured CO₂ mole~~
249 ~~concentration (μmol m⁻³), and the overline denotes the average value over a half-hour time period.~~
250 ~~A positive value of F_c indicates carbon emissions from the underlying surface during the given~~
251 ~~time interval, while a negative value represents carbon uptake.~~

252 The acquired 10 Hz raw data was processed and corrected using the EddyPro software
253 (EddyPro 7.06, Li-Cor, USA). The ~~calibration process~~~~correction process~~ involved outlier detection
254 for flux data, lag elimination, coordinate rotation (Jia et al., 2020), ultrasonic temperature
255 correction (Schotanus et al., 1983), frequency correction (Moncrieff et al., 1997), and
256 Webb-Pearman-Leuning (WPL) correction (Leuning and King, 1992), After these controls, the
257 integrity of the effective FC raw valid data we obtained reached 92.95 %. We removed outliers
258 caused by environmental disturbances such as power outages, rain, snow, and dust particles that
259 interfered with the instrument. Due to the slope of the underlying surface being around 5 degrees,
260 we also corrected from non-uniform and non-flat surfaces using EddyPro for double coordinate
261 rotation (Cao et al., 2019). ~~We also corrected errors resulting from non-uniform and non-flat~~
262 ~~underlying surfaces (Cao et al., 2019).~~As a result, we obtained half-hourly flux data with
263 associated data quality indicators. To evaluate the turbulence steadiness, we employed the "0-1-2"
264 quality assessment method, which classified flux results into three quality levels: 0 for excellent
265 data quality, 1 for moderate data quality, and 2 for low data quality (Mauder and Foken, 2011;
266 Foken et al., 2005)(Mauder and Foken, 2011). We removed data points labeled with a quality level
267 of "2". We further eliminated flux data with negative values during nighttime since plants do not
268 perform photosynthesis at night. Additionally, we conducted spectral analysis to identify and
269 remove data points with values significantly deviating from normal. Finally, friction velocities (u^*)
270 for each of the two years were determined separately using the method of moving point, and
271 deleted data recorded during nighttime when u^* was less than 0.28 and 0.39 $m s^{-1}$ (Reichstein et al.,
272 2005). After excluding outliers from the data, the data integrity is 72.67%. Tovi software (Tovi,
273 Li-Cor, USA) was used in the process.~~Finally, we utilized the friction velocity (U^*) as a criterion~~
274 ~~and deleted data recorded during nighttime when U^* was less than 0.28 and 0.39 $m s^{-1}$ (Papale et~~
275 ~~al., 2006).~~

276 When turbulence is weak, a portion of CO_2 is stored in the vegetation canopy and the
277 atmosphere below the measurement height. At this time, the NEE is calculated as (Zhang et al.,
278 2018):NEE of CO_2 can be represented by the following:

279
$$NEE = F_c + F_s \quad (2)$$

280 Where NEE represents the net ecosystem exchange of CO₂, F_c stands for the observed flux during
281 a specific period, F_s represents the CO₂ storage in the forest canopy, F_s is calculated as (Δc/Δt)·h,
282 where Δc is the difference in CO₂ concentration between two consecutive measurements, Δt is the
283 time interval between two consecutive measurements, and h is 35m.

284 We adopted the following formula as a gap-filling strategy for daytime NEE (NEE_{day})
285 concerning PAR, aiming to address missing values during the daytime (Falge et al., 2001):

286 ~~Where NEE represents the net ecosystem exchange of CO₂, F_c stands for the observed flux during~~
287 ~~a specific time period, F_s represents the CO₂ storage in the forest canopy, which is assumed to be~~
288 ~~zero in this case.~~

289 ~~We used the Michaelis-Menten model to fit the daytime NEE (NEE_{day}) with respect to PAR~~
290 ~~to fill in the missing values during the daytime (Falge et al., 2001):~~

$$291 \quad NEE_{\text{day}} = \frac{\alpha \cdot PAR \cdot P_{\text{max}}}{\alpha \cdot PAR + P_{\text{max}}} - R_{\text{day}} \quad (3)$$

292 where: α ($\mu\text{mol CO}_2/\mu\text{mol PAR}$) represents the apparent photosynthetic quantum efficiency, which
293 characterizes the maximum efficiency of converting light energy during photosynthesis. PAR
294 ($\mu\text{mol m}^{-2} \text{ s}^{-1}$) is the photosynthetically active radiation, a measure of the amount of light energy
295 available for photosynthesis. P_{max} ($\mu\text{mol CO}_2 \text{ m}^{-2} \text{ s}^{-1}$) is the apparent maximum photosynthetic rate,
296 representing the maximum CO₂ uptake rate under optimal conditions. R_{day} ($\mu\text{mol CO}_2 \text{ m}^{-2} \text{ s}^{-1}$) is
297 the daytime dark respiration rate, which denotes the rate of CO₂ release during daylight hours. The
298 parameters α , α , P_{max} , and R_{day} are obtained through the non-linear fitting of the Michaelis-Menten
299 model to the observed data.

300 During the nighttime, the NEE is modeled using an exponential function of ecosystem
301 respirationrespiration and soil temperature to fill in the missing values of NEE during the night
302 (NEE_{night}) (Lloyd and Taylor, 1994; Kato et al., 2006):

$$303 \quad NEE_{\text{night}} = a \cdot \exp^{(bt)} \quad (4)$$

304 The parameters a and b are estimated values for the exponential function used in modeling
305 NEE_{night}. The variable t represents the soil temperature measured at the depth of 5 cm. Origin 2023
306 (Originlab Corporation, USA) is the data processing software used for this analysis. For the
307 missing data, interpolation was performed using Tovi software allows for data interpolation to fill

308 ~~in the gaps~~The data processing software used for this analysis is Origin 2023 (Originlab
309 Corporation, USA). For the missing data, interpolation was performed using Tovi software (Tovi,
310 Li-Cor, USA) that allows for data interpolation to fill in the gaps and ensure a continuous dataset
311 for further analysis (Reichstein et al., 2005). 27.33% of missing data were interpolated, The final
312 flux data achieved a data integrity of 100%.

313 In flux analysis, the significance of source area contributions cannot be overlooked. In this
314 study, the peak distances of the 90% flux contribution areas averaged over two years are 364.2 and
315 357.1m, respectively. Looking at seasons, the average peak distances of the 90% flux contribution
316 areas for winter, spring, summer, and autumn over the two years are 353.9, 358.2, 350.05, and
317 344.34m, respectively.

318 2.4 Flux partitioning~~Flux splitting~~

319 Ecosystem respiration (RE) is the sum of plant and heterotrophic respiration in an ecosystem
320 and is obtained by adding the measured nighttime data to the extrapolated daytime data. Gross
321 primary productivity (GPP) is the total amount of organic carbon fixed by green plants through
322 photosynthesis per unit of time and per unit of area:

$$323 \text{RE} = \text{R}_{\text{day}} + \text{R}_{\text{night}} \quad (5)$$

$$324 \text{GPP} = -\text{NEE} + \text{RE} \quad (6)$$

325 Carbon use efficiency (CUE) is a crucial parameter that reflects the ability of an ecosystem to
326 sequester carbon. It is defined as the ratio of net ecosystem productivity (NEP) to gross primary
327 productivity.~~It is defined as the ratio of net primary productivity to gross primary productivity.~~
328 CUE can be expressed using the following equation:

$$329 \text{CUE} = \frac{\text{NEP}}{\text{GPP}} = \frac{-\text{NEE}}{\text{GPP}} \quad (7)$$

330 To study the variation of ecosystem respiration rates with environmental
331 factors~~environmental conditions~~, we considered the dependence of nocturnal ecosystem
332 respiration on soil temperature (Pavelka et al., 2007; Mamkin et al., 2023):

$$333 \text{Q}_{10} = \exp(10 \cdot \alpha) \quad (8)$$

$$334 \ln(\text{NEE}_{\text{night}}) = \alpha \cdot T + \gamma \quad (9)$$

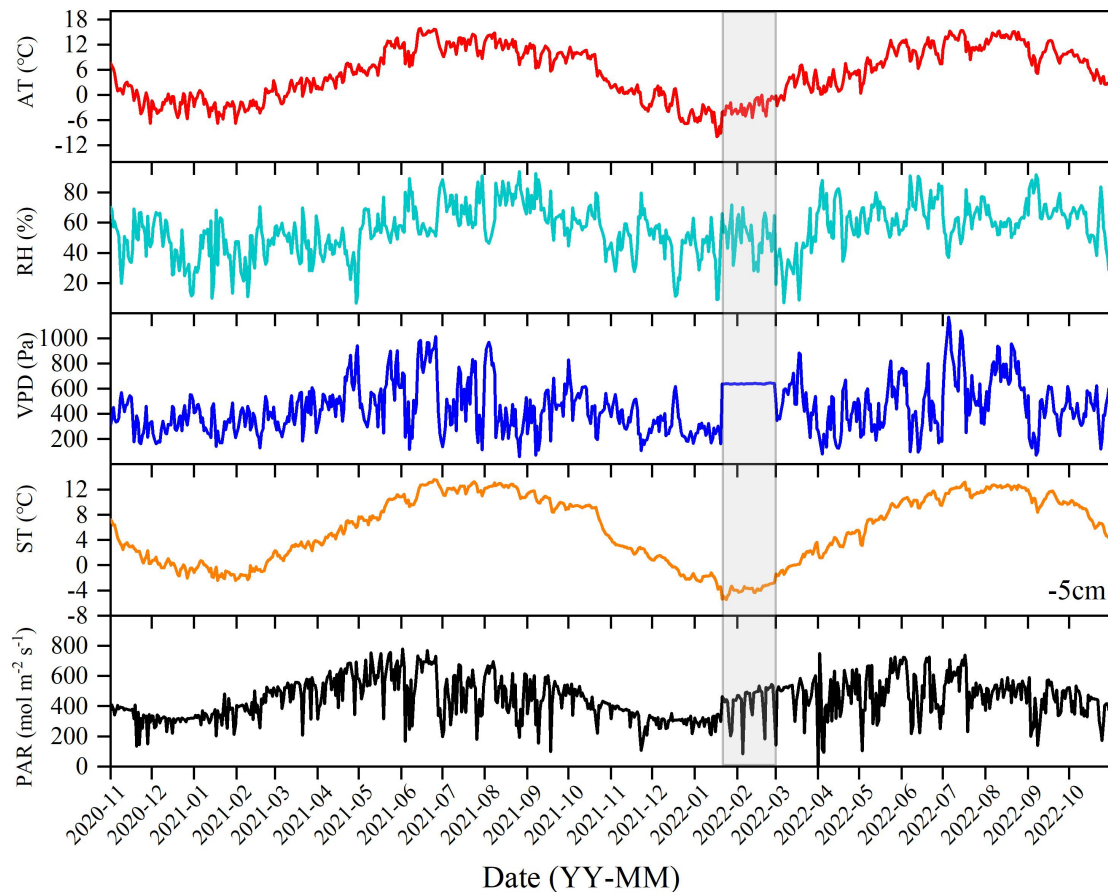
335 Where T is the soil temperature (°C) and γ is an empirical parameter of the equation.

336 To clarify the carbon sink potential of forests in the QTP and to compare it with other
337 ecosystems, a search was conducted in two authoritative databases, Web of Science and China
338 National Knowledge Internet, for research articles on the current utilization of EC systems in the
339 QTP. A total of 82 research results were collected from 48 studies, and their annual average
340 environmental factors, such as air temperature, precipitation, and altitude, were obtained.

341 **3 Results**

342 3.1 Daily average changes in main environmental factors

343 During the observational period, the environmental conditions exhibited significant
344 fluctuations. The winter and spring seasons were characterized by cold and dry conditions, while
345 the summer and autumn seasons were warm and humid. The daily maximum air temperature (AT)
346 recorded was 15.87 °C (on June 15, 2021), and the minimum temperature was -9.88 °C (on
347 January 17, 2022), with an average of 5.5 °C over the two years. The relative humidity (RH) with
348 an annual average of 55.89%. The vapor pressure deficit (VPD) with an annual average of 4.46
349 hPa. Soil temperature (ST) exhibited a similar trend to air temperature. The highest observed soil
350 temperature was 13.53 °C (on June 27, 2021), while the minimum was -3.78 °C (on January 18,
351 2022), with an annual average of 6.11 °C. Photosynthetically active radiation (PAR) with an
352 annual average of 447.24 mol m⁻² s⁻¹.~~The relative humidity (RH) ranged from a maximum of~~
353 ~~93.98% (on August 26, 2021) to a minimum of 6.74% (on April 29, 2021), with an annual average~~
354 ~~of 55.89%. The vapor pressure deficit (VPD), which represents the difference between the~~
355 ~~saturated vapor pressure and the actual vapor pressure in the air, influences plant stomatal closure~~
356 ~~and regulates physiological processes such as transpiration and photosynthesis. The highest~~
357 ~~recorded VPD was 1169.8 hPa (on July 5, 2022), and the lowest one was 60.8 hPa (on August 26,~~
358 ~~2021), with an annual average of 446.4 hPa. Soil temperature (ST) exhibited a similar trend to air~~
359 ~~temperature and remained relatively stable over short periods. The highest observed soil~~
360 ~~temperature was 13.53 °C (on June 27, 2021), while the minimum was -3.78 °C (on January 18,~~
361 ~~2022), with an annual average of 6.11 °C. Photosynthetically active radiation (PAR) reached a~~
362 ~~maximum value of 779.06 mol m⁻² s⁻¹ (on June 2, 2021), with an annual average of 447.24 mol~~
363 ~~m⁻² s⁻¹. From March to October, the radiation conditions were favorable for photosynthesis, but~~
364 ~~reduction in radiation intensity was observed during rainy, snowy, and cloudy weather conditions.~~



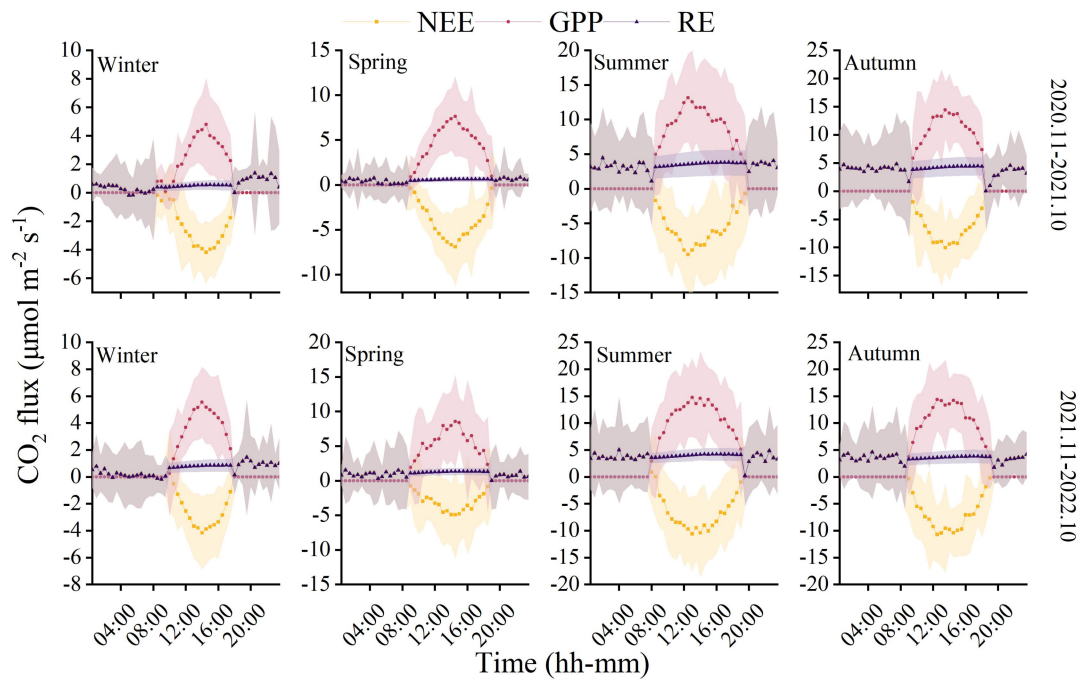
365

366 Figure 2. Daily values of main environmental factors, air temperature (AT), relative humidity
 367 (RH), vapor pressure deficit (VPD), soil temperature (ST), and Photosynthetically active radiation
 368 (PAR). (The data of the shadow part in the figure comes from the Ranwu forest site (Figure 1).
 369 Since there was no interpolated data source for VPD, the annual average was used instead.)(The
 370 shaded part of the figure represents the data interpolated by the nearby station)

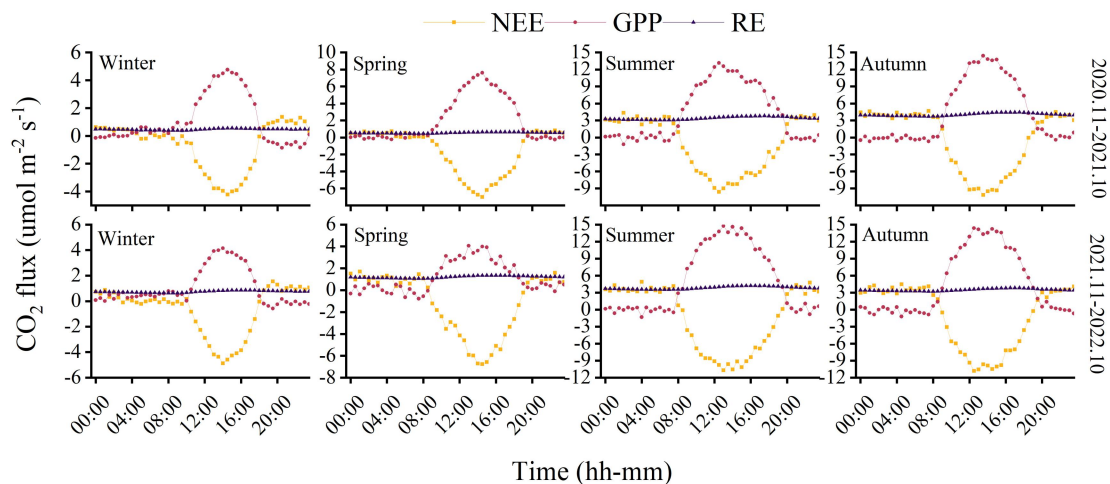
371 3.2 The seasonal variations in NEE, RE, and GPP

372 The observations from the forest ecosystem indicate distinct diurnal and seasonal variations
 373 in NEE and GPP. The NEE and GPP exhibit a pronounced U-shaped curve, with significant
 374 seasonal differences. The summer and autumn are characterized by peak carbon uptake, with the
 375 maximum NEE reaching ~~-10.78 $\mu\text{mol CO}_2\text{-m}^{-2}\text{-s}^{-1}$ (12:30, autumn)~~. During the nighttime, the
 376 ecosystem generally releases carbon, while during favorable daytime meteorological conditions, it
 377 demonstrates a carbon uptake capacity. The peak carbon absorption of the forest ecosystem occurs
 378 from 12:00 to 15:00 (Beijing time, UTC+8:00)~~(Beijing time, UTC+8:00)~~. daily carbon
 379 sequestration~~The carbon sequestration period~~ in summer and autumn is 1.5-3 hrs longer than in
 380 winter. The timing of maximum carbon sequestration capacity changes with each season. In

381 winter, the transition from nighttime carbon release to daytime carbon uptake occurs around 08:30,
382 which is approximately 1 hour later than in summer. GPP characterizes the forest's carbon
383 sequestration capacity, and since photosynthesis does not occur at night, GPP is zero during
384 nighttime. The maximum daily total productivity is recorded at $14.76 \pm 7.34 \mu\text{mol CO}_2 \text{ m}^{-2} \text{ s}^{-1}$
385 during the summer of the second year, with a standard deviation indicating greater variability in
386 GPP and NEE during the summer and autumn compared to the winter and spring. Although
387 diurnal variations in RE are relatively small, there are significant seasonal differences. During the
388 night, when only respiration occurs, RE equals NEE. However, as photosynthesis becomes active
389 during the day, RE gradually increases and stabilizes. The respiratory rate of the coniferous forest
390 is highest in autumn, being eight times greater than in winter.~~In winter, the transition from~~
391 ~~nighttime carbon release to daytime carbon uptake occurs around 08:30, while in summer, it shifts~~
392 ~~to around 07:30 (Beijing time, UTC+8:00). GPP reflects the carbon sequestration capacity of the~~
393 ~~forest, with the recorded daily total productivity highest at $14.76 \mu\text{mol CO}_2 \text{ m}^{-2} \text{ s}^{-1}$ during summer~~
394 ~~season of second year, RE exhibits minor diurnal variations but shows significant seasonal~~
395 ~~differences, with maximum and minimum diurnal RE values of $0.73 \mu\text{mol CO}_2 \text{ m}^{-2} \text{ s}^{-1}$ and 0.17~~
396 ~~$\mu\text{mol CO}_2 \text{ m}^{-2} \text{ s}^{-1}$, respectively. The respiration rate of the coniferous forest during the summer and~~
397 ~~autumn is 5-8 times higher than that in the winter and spring.~~



398



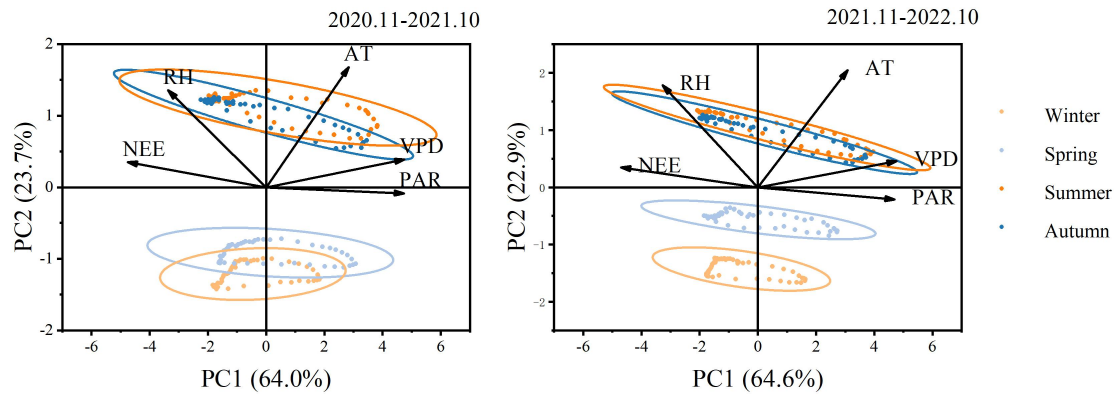
399

400 **Figure 3. Monthly mean values of carbon fluxes** ~~Figure 3 The monthly variations in carbon fluxes~~

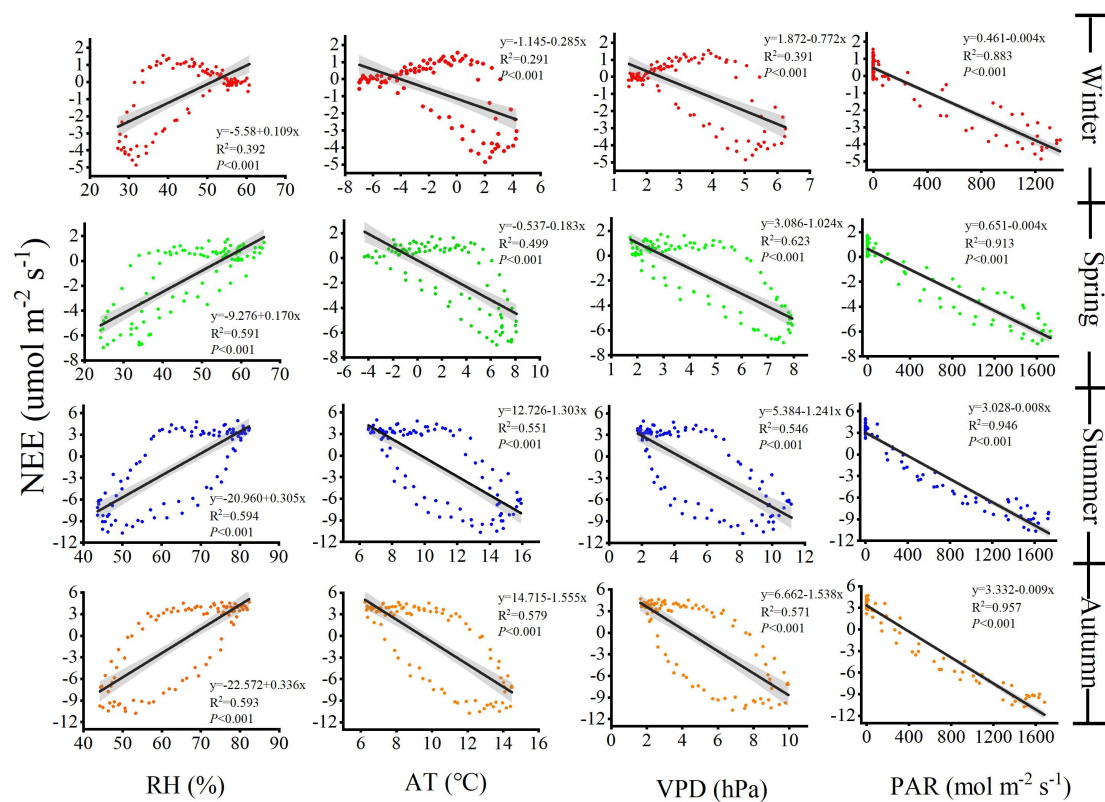
401 **3.3 Relationship between NEE and main environmental factors**

402 The PCA analysis of two years of NEE and environmental factors (Figure 4) indicates that
 403 the explanations for the first principal component (PC1) and the second principal component (PC2)
 404 are essentially the same between the two years. The total contributions of PC1 and PC2 are 87.7%
 405 and 87.5%, respectively, with PC1 accounting for 64.0% and 64.6% individually. The angle
 406 between photosynthetically active radiation (PAR) and PC1 is minimal, suggesting a strong
 407 correlation between PAR and PC1. Additionally, PAR and VPD contribute the most to PC1, while
 408 AT and RH contribute the most to PC2. The analysis results reveal a significant positive
 409 correlation between NEE and RH, while a significant negative correlation is observed with AT,

410 VPD, and PAR. This implies that an increase in RH is unfavorable for the forest's absorption of
411 carbon dioxide. Among these environmental factors, PAR plays a dominant role. Furthermore, the
412 figure illustrates the relationships between environmental factors, showing a positive correlation
413 between RH and TA, and a negative correlation with VPD and APR. The indicators exhibit some
414 seasonality, with notable differences between the winter-spring and summer-autumn seasons,
415 indicating limited similarity between seasons.~~The fitting results between NEE and environmental~~
416 ~~factors indicate that the selected environmental factors have a significant impact on NEE ($P < 0.001$)~~
417 ~~(Figure 4). However, the influence of individual environmental factors on NEE varies across~~
418 ~~different seasons. RH has the smallest impact on NEE during the summer, while AT, VPD, and~~
419 ~~PAR exhibit the strongest influence on NEE during the autumn. These factors consistently have~~
420 ~~the least impact on NEE during autumn. In the same season, PAR primarily controls NEE, with an~~
421 ~~R^2 value reaching up to 0.957. Positive values of NEE indicate carbon emissions, while negative~~
422 ~~values indicate carbon uptake. Therefore, air temperature, vapor pressure deficit, and PAR all~~
423 ~~have a significant positive effect on carbon uptake, while an increase in humidity leads to a~~
424 ~~noticeable reduction in carbon uptake.~~



425



426

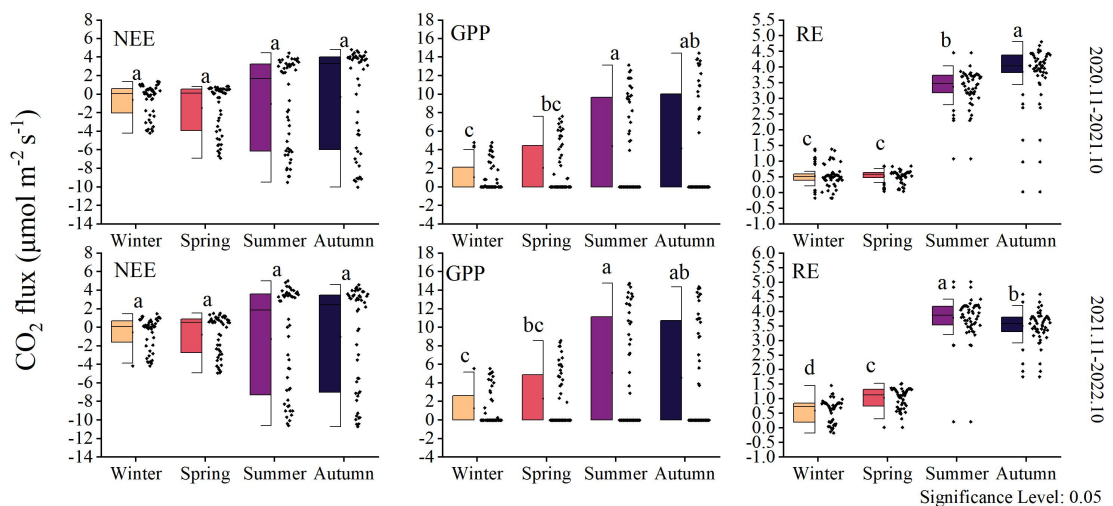
427 **Figure 4. Principal component analysis of environmental factors and NEE**

428 **Relationship between NEE and main environmental factors**

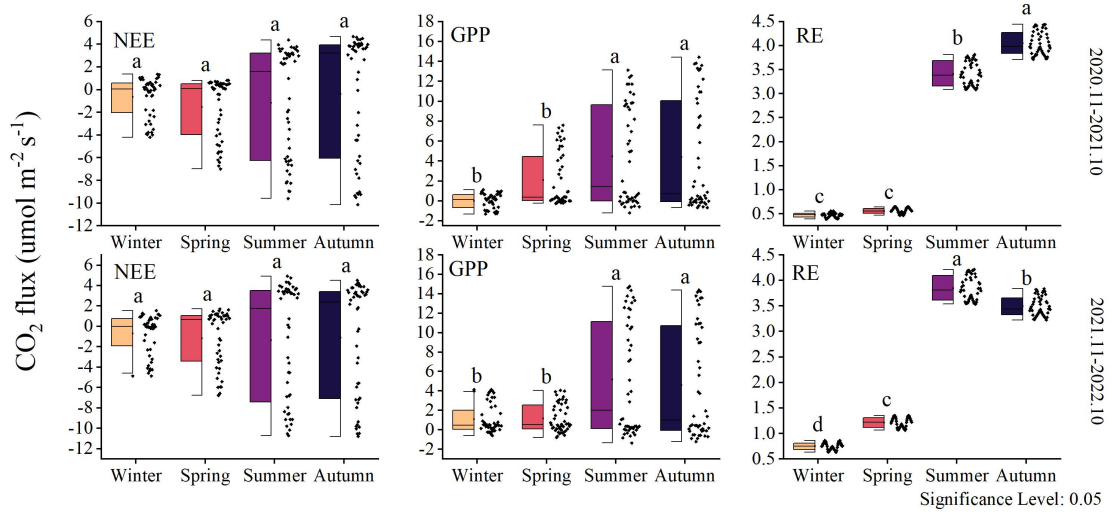
429 **3.4 Seasonal variation characteristics of NEE, GPP, and RE**

430 The NEE ~~rate~~ did not show significant inter-seasonal differences (Figure 5). However, data
 431 distribution indicates that the variability in NEE rate differs across different seasons, particularly
 432 between summer-autumn and winter-spring. However, data distribution indicates that the
 433 variability in NEE rate differs across different seasons, particularly between the growing seasons
 434 (summer, autumn) and the non-growing seasons (winter, spring). The changes in GPP over the
 435 two years were similar, with significant differences observed between summer and winter

436 ($P<0.05$). The RE was higher during summer-autumn compared to winter-spring. The highest
 437 ecosystem respiration occurred in the first year during autumn, while in the second year, it was
 438 highest during summer. Within the same year, summer and autumn exhibited significant
 439 differences ($P<0.05$), while between the same seasons in different years, notable distinctions were
 440 not observed, with significant differences observed between the growing seasons and the
 441 non-growing seasons ($P<0.05$). The RE was higher during the growing seasons compared to the
 442 non-growing seasons. The forest ecosystem respiration rate was lowest in winter and slightly
 443 higher in spring. The highest ecosystem respiration occurred in the first year during autumn, while
 444 in the second year, it was highest during summer. This pattern is also reflected in GPP and NEE.



445

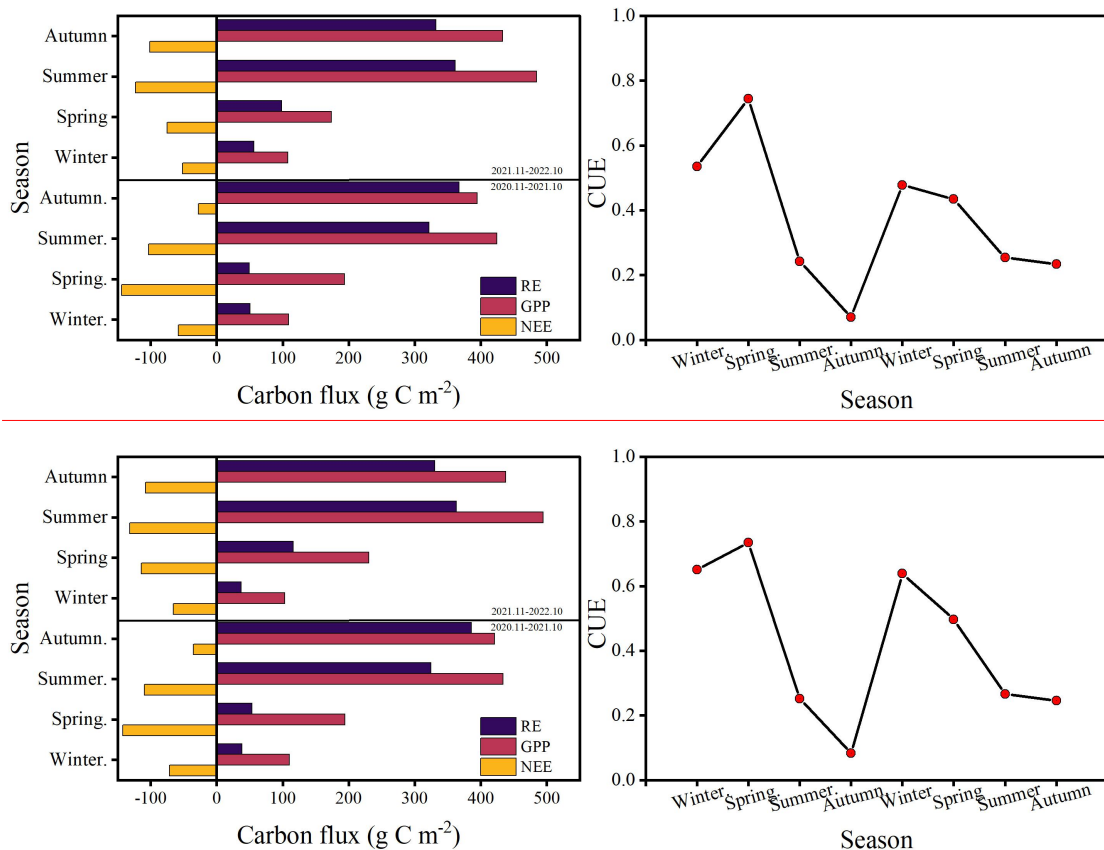


446

447 Figure 5. Seasonal variation of carbon fluxes

448 3.5 Changes in total NEE, GPP, RE, and CUE

449 The cumulative fluxes over the two years for the forest ecosystem are shown in Figure 6.
 450 NEE indicates the net carbon sequestration in each month. The cumulative respiration reached its
 451 highest value of 361 g C m⁻² in the summer of 2022. The total NEE, GPP, and RE for the first year
 452 were -332, 1121, and 788 g C m⁻², respectively, and -351, 1199, and 847 g C m⁻² for the second
 453 year, respectively. The CUE was higher during the spring and lower during the autumn, with a
 454 maximum value of 0.74 and a minimum value of 0.07. The average CUE over the two years was
 455 0.40 and 0.35, respectively.~~The cumulative respiration reached its highest value of 363.23 g C m⁻²~~
 456 ~~in the summer of 2022.~~ The total NEE, GPP, and RE for the first year were ~~-358.65, 1159.60, and~~
 457 ~~802.67 g C m⁻², respectively, and -419.41, 1265.96, and 846.55 g C m⁻² for the second year,~~
 458 ~~respectively.~~ The CUE was higher during the cold non-growing seasons and lower during the
 459 ~~growing seasons, with a maximum value of 0.73 and a minimum value of 0.08.~~ The average CUE
 460 ~~over the two years was 0.43 and 0.41, respectively.~~



461
 462
 463 Figure 6. Change in total carbon flux and carbon use efficiency

464 3.6 The carbon sequestration potential of subalpine forests of QTP

465 To clarify the carbon sequestration contribution of the subalpine forests found in the QTP, we
466 compared these research results (Figure 7). Found that ecosystems with high vegetation cover
467 exhibited higher annual cumulative carbon sequestration. Among these ecosystems, the subalpine
468 forests in the QTP showed the highest carbon sequestration potential, reaching an average of
469 ~~368391.48~~ 368391.48 g C m² per year. The carbon sequestration potential of different ecosystems ranked as
470 follows: forest > meadow > steppe > shrub. The average value for wetlands indicated that they are
471 a significant source of CO₂, releasing ~~5756.93~~ 5756.93 g C m⁻² into the atmosphere annually. We also
472 analyzed the influence of altitude, mean annual air temperature, and precipitation on NEE at these
473 sites in the QTP. It has been observed that these sites cover a wide range of altitudes, ranging from
474 1977 to 4800 m. According to existing results, an increase in elevation may lead to a reduction in
475 carbon uptake, while the range of mean annual temperature varies between -14.8 to 15.1 °C, and
476 higher mean annual temperatures significantly increase carbon uptake. Forests exhibit the highest
477 mean annual precipitation, averaging 827 mm, with mean annual precipitation having a relatively
478 weak impact on the NEE. It was found that increasing elevation had a negative impact on carbon
479 uptake, while higher mean annual temperatures significantly increased carbon uptake. Mean
480 annual precipitation had a weak influence on NEE. These findings highlight the important role of
481 subalpine forests in carbon sequestration in the QTP and provide insights into the factors that
482 affect carbon exchange in the QTP, such as altitude, temperature, and precipitation.

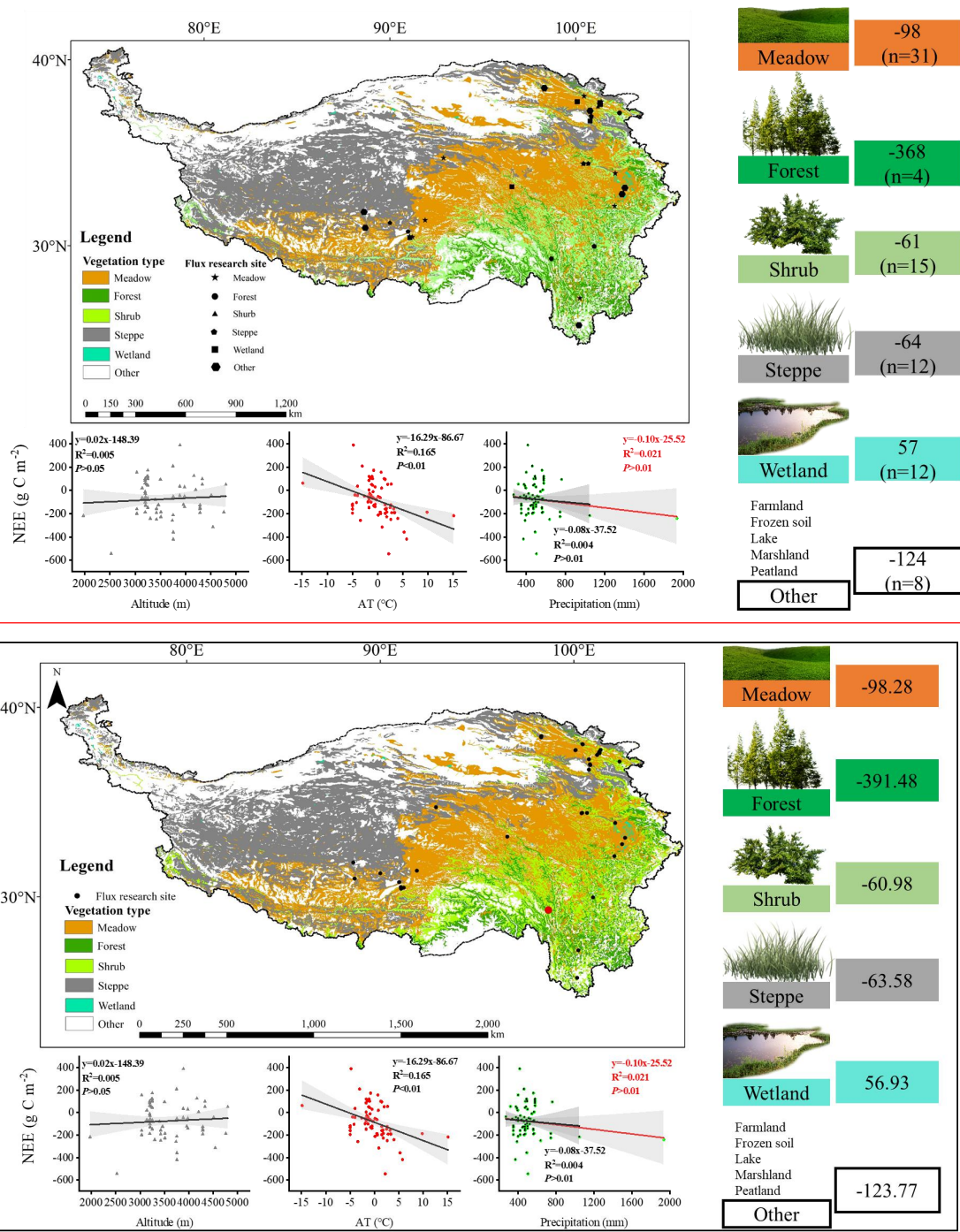


Figure 7. Carbon exchange potential of different ecosystems in the Qinghai-Tibet Plateau

4 Discussion

4.1 Main factors affecting the carbon sequestration function of subalpine forests

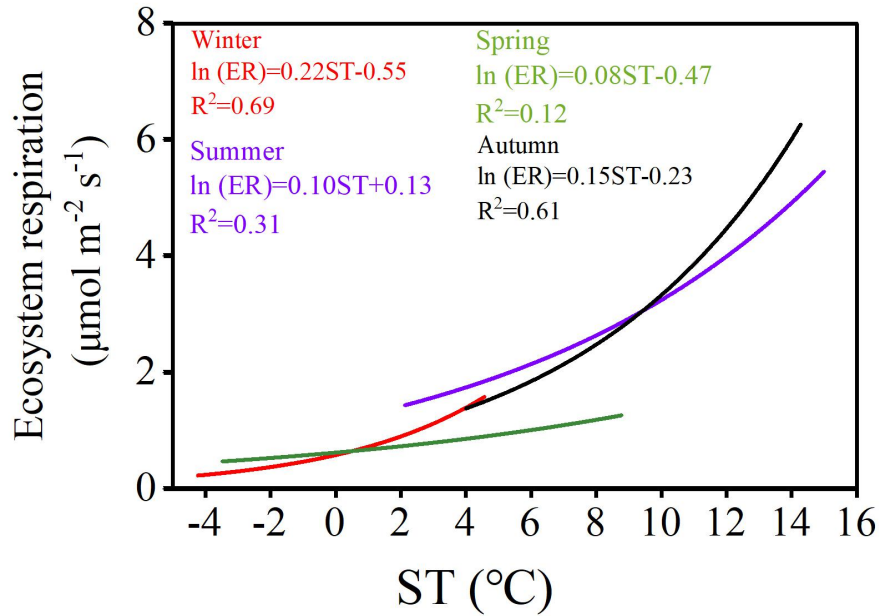
Climate change significantly affects the vegetation's carbon sequestration capacity, particularly at the seasonal scale due to phenological changes (Acosta-Hernández et al., 2020). In the short term, these factors (PAR, AT, RH, and VPD) play important roles in regulating vegetation photosynthesis and, consequently, carbon uptake. For instance, PAR representing the

492 portion of solar energy that can be utilized by plants and is an essential component in chloroplast
493 reactions. PAR drives a nonlinear response of GPP to Solar-induced fluorescence (SIF) across
494 different seasons, resulting in a strong positive correlation between GPP and SIF (Wang et al.,
495 2023b). VPD affects photosynthesis and transpiration of leaves, with stomata serving as tiny pores
496 mediating carbon dioxide uptake. Research has demonstrated that excessive increases in VPD are
497 detrimental to photosynthesis. For instance, a moderate increase in VPD significantly reduces
498 photosynthetic efficiency under light fluctuations , due to changes in RH and/or AT often
499 accompany fluctuations in light, studies also indicate that the impact of VPD on sunlight
500 utilization efficiency is primarily determined by relative RH rather than AT (Liu et al., 2024). In
501 different seasons, the same influencing factors exhibit varying degrees of contribution to NEE. For
502 example, during winter, when the climatic conditions are relatively harsh with low air temperature
503 and humidity, the forest maintains a low level of carbon uptake. Climate change is the significant
504 factor affecting the vegetation's carbon sequestration capacity, particularly at the seasonal scale
505 due to phenological changes (Acosta-Hernández et al., 2020). Our study has demonstrated that, in
506 the short term, NEE is primarily influenced by factors such as PAR, AT, RH, and VPD. These
507 factors play a role in regulating vegetation photosynthesis and, consequently, carbon uptake. For
508 instance, PAR represents the portion of solar energy that can be utilized by plants and is an
509 essential component in chloroplast reactions. AT regulates the activity of enzymes involved in
510 light and dark reactions, which may contribute to seasonal variations in NEE. RH and VPD impact
511 the entire process of photosynthesis by influencing the concentration of CO₂ in the air and the
512 stomatal conductance (the pathway for CO₂ exchange). In different seasons, the same influencing
513 factors exhibit varying degrees of contribution to NEE. For example, during winter, when the
514 climatic conditions are relatively harsh with low air temperature and humidity, the forest
515 maintains a low level of carbon uptake. While the forest continues to absorb carbon dioxide, the
516 uptake remains limited at a low level under such unfavorable conditions. On longer time scales,
517 such as annual and decadal variations, the inherent changes in forest NEE may be attributed to
518 disturbances and recovery (Hayek et al., 2018). In this study, significant differences in ecosystem
519 respiration were observed during the summer and autumn in different years. Past research
520 suggested that due to leaf aging or water stress, the photosynthetic light use efficiency of the

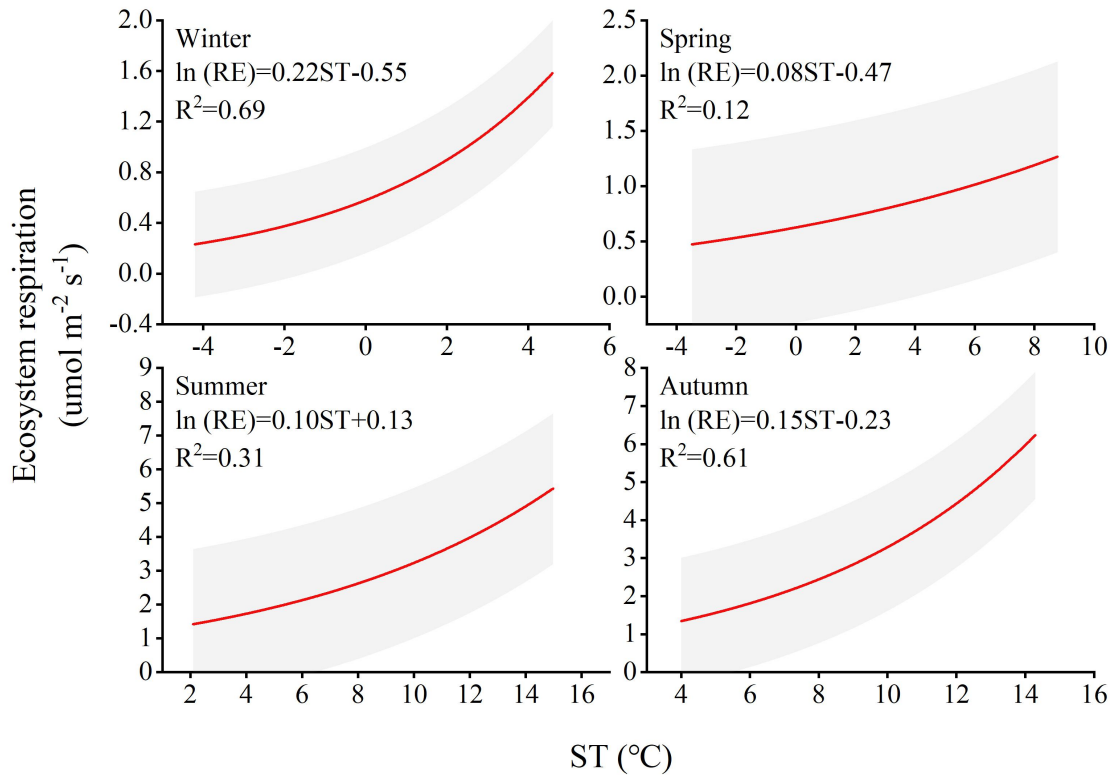
521 ecosystem peaks after spring leaf expansion and gradually declines (Wehr et al., 2016). This
522 implies a peak in carbon exchange during the summer, followed by higher productivity and
523 ecosystem respiration in the following seasons. The variation in different years may be attributed
524 to rainfall regulating the availability of natural resources such as water, biomass, litter, and soil
525 nutrients (Schwinning and Sala, 2004). For instance, in temperate forests, when microbial biomass
526 undergoes seasonal changes, microbial activity exhibits a seasonal lag in response to temperature
527 variation, resulting in a seasonally delayed effect between litter heterotrophic respiration and
528 temperature (Ataka et al., 2020). Whether such differences persist between different years on
529 longer time scales remains to be demonstrated through more sustained and detailed research in the
530 future. Ecosystem respiration~~Research by Amiro (2001) has demonstrated that disturbances~~
531 ~~caused by fire and logging have been found to regulate the carbon balance of northern forests in~~
532 ~~Canada over several decades. Additionally, there are close relationships between subtle climate~~
533 ~~changes, stand dynamics, tree age, post-disturbance time, and forest carbon storage and cycling~~
534 ~~(Bradford et al., 2008). Compared to naturally regenerating forests, actively restored forests~~
535 ~~exhibit higher rates of carbon accumulation. Restoration efforts have been shown to increase~~
536 ~~aboveground carbon density recovery rates by more than 50% over a decade, from 2.9 to 4.4~~
537 ~~megagrams per hectare per year (Philipson et al., 2020). The carbon dioxide generated by soil~~
538 ~~microbial activity is an essential component of forest ecosystem respiration. Soils contain the~~
539 ~~largest organic carbon reservoir on Earth, three times more than the carbon content in the~~
540 ~~atmosphere (Tifafi et al., 2018). With climate warming, soil microorganisms, and root systems~~
541 ~~will decompose soil organic carbon at a faster rate, releasing carbon dioxide into the atmosphere~~
542 ~~more rapidly. Temperature plays a more sensitive role in soil carbon turnover in cold climate~~
543 ~~regions compared to warmer conditions (Koven et al., 2017). Ecological respiration~~ sensitivity to
544 temperature is represented by the Q_{10} coefficient. In this study, seasonal variations influenced the
545 magnitude of Q_{10} (as shown in Figure 8). The calculated Q_{10} for each season are as follows: 9.025,
546 2.22, 2.71, and 4.48. The winter season exhibited the highest sensitivity of forest ecosystem
547 respiration to temperature, indicating that respiration rates in the winter are more responsive to
548 changes in temperature compared to other seasons. The main reason for such differences is that
549 ecosystem respiration consists of heterotrophic respiration and autotrophic respiration, which are

550 typically governed by different factors (Edwards, 1975). For instance, the high activity of soil
551 microbes contributes to heterotrophic respiration, a process dominated by soil temperature and
552 moisture conditions, which are severely restricted during the cold and dry conditions of winter
553 (Falge et al., 2002). Simultaneously, due to the changing relative roles of growth and maintenance
554 respiration, the allocation of autotrophic respiration varies seasonally. In winter, soil CO₂
555 emissions constitute a significant portion of ecosystem CO₂ emissions, and in some boreal forests,
556 the ratio between the two can reach 0.6 or even higher (Davidson et al., 2006). In winter, under the
557 frequent coverage of snow, cold-adapted microorganisms thriving in a relatively narrow sub-zero
558 temperature range engage in respiration and exhibit relatively high sensitivity to warming or
559 cooling beyond this range (Monson et al., 2006). The seasonal patterns of the Q₁₀ value are jointly
560 determined by the variation in the ratio of soil respiration to ecosystem respiration, reflecting these
561 seasonal changes. The winter season exhibited the highest sensitivity of forest ecosystem
562 respiration to temperature, indicating that respiration rates in the winter are more responsive to
563 changes in temperature compared to other seasons.

564 Our integrated analysis (as shown in Figure 7) reveals that despite the high elevation of the
565 "Third Pole", the topographic factor of elevation does not have a significant impact on carbon
566 uptake. Instead, NEE gradually increases with a steep rise in elevation. Research conducted by
567 Wang et al. (2023c)WANG et al.(2023b), indicates that mean annual average temperature and
568 precipitation are the main driving factors of interannual variations in NEE in alpine meadows and
569 alpine steppes. Decreased precipitation resulting in a transition into carbon sources at some
570 regions with high precipitation-dependent alpine grasslands. It is worth noting that, among all data
571 collection sites, alpine wetlands show an average carbon source trend. Due to prolonged flooding
572 and low temperatures, microbial activity in alpine wetlands is hindered, and the accumulation of
573 organic carbon from plant litter decomposition is substantial. As a result, approximately 5756.93 g
574 C m⁻² is emitted into the atmosphere annually. Previous studies have indicated that NEE in alpine
575 wetlands is increasing with global warming (Yasin et al., 2022).



576



577

578 Figure 8. Relationship between NEEnight and soil temperature in different seasons

579 4.2 Sustained carbon sequestration of subalpine forests

580 Subalpine forests are integral components of global alpine ecosystems and play crucial roles
 581 in the global carbon cycle. Our study on subalpine forests demonstrates a continuous absorbing of
 582 carbon dioxide even during winter, which aligns well with measurements taken in the vicinity of
 583 Mount Fuji in Japan (Mizoguchi et al., 2012). The age of subalpine forests is a crucial factor

584 influencing sustained carbon sequestration. Based on NPP simulations of natural subalpine forests
585 in the Northern Rockies, Carey. (2001) found that aboveground net primary productivity reaches
586 its maximum after approximately 250 years, followed by a decline, this challenges the previous
587 view that forests older than 100 years are generally considered to be unimportant carbon sinks.
588 Compared to the forest (mature forest) of Mount Gongga in the QTP (e.g., Zhang et al., 2018), the
589 subalpine forest in this study exhibits a stronger carbon sequestration capacity. However, its
590 carbon sequestration ability is slightly weaker than that of the Qilian Mountains high-mountain
591 forests (approximately 60-70 years old) in the QTP (Zhang et al., 2018; Du et al., 2022b).
592 Although existing flux monitoring results of high-altitude forests in the QTP indicate that these
593 forest ecosystems act as carbon sinks, it is important to consider that globally there are still many
594 cold regions with coniferous forests serve as carbon sources. For example, continuous CO₂ flux
595 monitoring from native boreal forests in Sweden for over 10 years indicates that they are a net
596 carbon source, which is attributed to the contribution of woody debris to RE due to disturbances
597 such as extreme weather events, fires, insect infestations, and pathogen attacks (Hadden and
598 Grelle, 2017). In the summer of 2018, Europe experienced a heatwave that affected the carbon
599 cycling in forests. The mixed coniferous-deciduous forest in southern Estonian, under the
600 influence of the heatwave, transitioned from a net carbon sink to a net carbon source in 2018
601 (Krasnova et al., 2022). Particular attention should be paid to the long-term monitoring in
602 high-altitude environments of the impact of disturbances on forest carbon sequestration capacity.
603 Our study has shown that forests in the QTP have the strongest carbon sink capacity, indicating
604 that alpine forests will have an important sustained effect on carbon reduction in the QTP in the
605 context of future climate change, but whether this sustained effect will be longer than other
606 ecosystems is still unknown. However, a modeling experiment in a large semi-arid area of
607 California predicted that grasslands are more resilient carbon sinks than forests in responding to
608 climate change in the 21st century (Dass et al., 2018). In terms of carbon sequestration rate, forests
609 in the QTP were significantly stronger than other ecosystems, followed by grasslands, while
610 alpine deserts and alpine grasslands in the north-western and southern regions were the main
611 carbon sources (Wu et al., 2022). Forests are mostly distributed in the south-eastern margin of the
612 QTP and the mid-altitude area near 3000 m in the Sichuan-Tibet alpine gorge area, with an area of

613 | $19.3 \times 10^4 \text{ km}^2$ (Yu et al., 2022)(Y et al., 2022). Based on the average value of a few current
614 carbon flux monitoring, the forest in the QTP will absorb about $71 \times 10^6 \text{ Mg C year}^{-1}$.

615 **5 Conclusion**

616 This study explores the carbon sequestration function, seasonal variations, and climate
617 drivers of subalpine forests in the QTP. Over the observational period, We synchronously
618 monitored ecosystem carbon exchange and primary environmental factors using an eddy
619 covariance system. The research reveals that the subalpine forest is a carbon sink, with a total
620 NEE, GPP, and RE of -332, 1121, and 788 g C m⁻², respectively, and -351, 1199, and 847 g C m⁻²
621 for two years, respectively.~~with a total NEE, GPP, and RE of -358.65, 1159.60, and 802.67 g C~~
622 ~~m⁻², respectively, and -419.41, 1265.96, and 846.55 g C m⁻² for two years, respectively.~~
623 Photosynthetically active radiation was identified as the primary control of NEE. The NEE did not
624 exhibit significant differences across seasons. Combining results from other eddy covariance sites
625 on the QTP, this study highlights those forests have the highest carbon sequestration potential,
626 reaching 368 g C m^{-2} annually, followed by meadows, steppes, and shrubs. Wetlands, however,
627 were identified as a substantial carbon dioxide source. Despite the challenges posed by climate
628 change, the subalpine forests in the QTP retain substantial carbon sequestration potential.
629 Strengthening conservation and management efforts for subalpine forests is crucial to ensure their
630 continued and significant carbon sequestration function in the future. Overall, this research
631 underscores the vital role of subalpine forests in the QTP as essential carbon sink regions, playing
632 a critical role in the context of global climate change.

633 ***Data availability.*** The data is available from the authors on request.

634 ***Authorship contributions.*** Niu Zhu: Conceptualization, study design, data analyses,
635 visualization, writing-original draft. JinNiu Wang: study design, writing—review & editing,
636 supervision, project administration, funding acquisition. Dongliang Luo and Xufeng Wang:
637 writing-reviewing & editing. Cheng Shen and Ning Wu: resources, data curation, supervision. all
638 authors approved the final manuscript.

639 ***Declaration of competing interest.*** The authors declare that they have no conflict of interest.

640 **Acknowledgements.** We thank Ms. Neha Bisht for her substantial comments and language
641 revision on improving the manuscript. This study was funded by CAS "Light of West China"
642 Program (2021XBZG-XBQNXXZ-A-007); National Natural Science Foundation of China
643 (31971436); State Key Laboratory of Cryospheric Science, Northwest Institute of
644 Eco-Environment and Resources, Chinese Academy Sciences (SKLCS-OP-2021-06).

645 **Reference**

646 Acosta-Hernández, A. C., Padilla-Martínez, J. R., Hernández-Díaz, J. C., Prieto-Ruiz, J. A.,
647 Goche-Telles, J. R., Nájera-Luna, J. A., and Pompa-García, M.: Influence of Climate on Carbon
648 Sequestration in Conifers Growing under Contrasting Hydro-Climatic Conditions, *Forests*, 11, 1134,
649 2020.

650 Ataka, M., Kominami, Y., Sato, K., and Yoshimura, K.: Microbial Biomass Drives Seasonal Hysteresis
651 in Litter Heterotrophic Respiration in Relation to Temperature in a Warm-Temperate Forest, *Journal of*
652 *Geophysical Research: Biogeosciences*, 125, e2020JG005729, <https://doi.org/10.1029/2020JG005729>,
653 2020.

654 Banbury Morgan, R., Herrmann, V., Kunert, N., Bond-Lamberty, B., Muller-Landau, H. C., and
655 Anderson-Teixeira, K. J.: Global patterns of forest autotrophic carbon fluxes, *Global Change Biology*,
656 27, 2840-2855, <https://doi.org/10.1111/gcb.15574>, 2021.

657 Baumgartner, S., Barthel, M., Drake, T. W., Bauters, M., Makelele, I. A., Mugula, J. K., Summerauer,
658 L., Gallarotti, N., Cizungu Ntaboba, L., Van Oost, K., Boeckx, P., Doetterl, S., Werner, R. A., and Six,
659 J.: Seasonality, drivers, and isotopic composition of soil CO₂ fluxes from tropical forests of the Congo
660 Basin, *Biogeosciences*, 17, 6207-6218, 10.5194/bg-17-6207-2020, 2020.

661 Cai, W., He, N., Li, M., Xu, L., Wang, L., Zhu, J., Zeng, N., Yan, P., Si, G., and Zhang, X.: Carbon
662 sequestration of Chinese forests from 2010 to 2060: Spatiotemporal dynamics and its regulatory
663 strategies, *Science Bulletin*, 67, 836-843, 2022.

664 Cao, S., Cao, G., Chen, K., Han, G., Liu, Y., Yang, Y., and Li, X.: Characteristics of CO₂, water vapor,
665 and energy exchanges at a headwater wetland ecosystem of the Qinghai Lake, *Canadian Journal of Soil*
666 *Science*, 99, 227-243, 10.1139/cjss-2018-0104, 2019.

667 Carey, E. V., Sala, A., Keane, R., and Callaway, R. M.: Are old forests underestimated as global carbon
668 sinks?, *Global Change Biology*, 7, 339-344, 10.1046/j.1365-2486.2001.00418.x, 2001.

669 Chen, H., Ju, P. J., Zhu, Q., Xu, X. L., Wu, N., Gao, Y. H., Feng, X. J., Tian, J. Q., Niu, S. L., Zhang, Y.
670 J., Peng, C. H., and Wang, Y. F.: Carbon and nitrogen cycling on the Qinghai-Tibetan Plateau,
671 NATURE REVIEWS EARTH & ENVIRONMENT, 3, 701-716, 10.1038/s43017-022-00344-2, 2022.

672 Cole, J. J., Caraco, N. F., Kling, G. W., and Kratz, T. K.: Carbon dioxide supersaturation in the surface
673 waters of lakes, Science, 265, 1568-1570, 1994.

674 Dass, P., Houlton, B. Z., Wang, Y., and Warlind, D.: Grasslands may be more reliable carbon sinks than
675 forests in California, Environmental Research Letters, 13, 074027, 10.1088/1748-9326/aacb39, 2018.

676 Davidson, E. A., Richardson, A. D., Savage, K. E., and Hollinger, D. Y.: A distinct seasonal pattern of
677 the ratio of soil respiration to total ecosystem respiration in a spruce-dominated forest, Global Change
678 Biology, 12, 230-239, <https://doi.org/10.1111/j.1365-2486.2005.01062.x>, 2006.

679 Du, C., Zhou, G., and Gao, Y.: Grazing exclusion alters carbon flux of alpine meadow in the Tibetan
680 Plateau, Agricultural and Forest Meteorology, 314, 108774, 2022a.

681 Du, Y., Pei, W., Zhou, H., Li, J., Wang, Y., and Chen, K.: Net ecosystem exchange of carbon dioxide
682 fluxes and its driving mechanism in the forests on the Tibetan Plateau, Biochemical Systematics and
683 Ecology, 103, 10.1016/j.bse.2022.104451, 2022b.

684 Ebermayer, E.: Die gesammte Lehre der Waldstreu mit Rücksicht auf die chemische Statik des
685 Waldbaues: unter Zugrundlegung der in den Königl. Staatsforsten Bayerns angestellten
686 Untersuchungen, Springer1876.

687 Edwards, N. T.: Effects of Temperature and Moisture on Carbon Dioxide Evolution in a Mixed
688 Deciduous Forest Floor, Soil Science Society of America Journal, 39, 361-365,
689 <https://doi.org/10.2136/sssaj1975.03615995003900020034x>, 1975.

690 Falge, E., Baldocchi, D., Tenhunen, J., Aubinet, M., Bakwin, P., Berbigier, P., Bernhofer, C., Burba, G.,
691 Clement, R., Davis, K. J., Elbers, J. A., Goldstein, A. H., Grelle, A., Granier, A., Guðmundsson, J.,
692 Hollinger, D., Kowalski, A. S., Katul, G., Law, B. E., Malhi, Y., Meyers, T., Monson, R. K., Munger, J.
693 W., Oechel, W., Paw U, K. T., Pilegaard, K., Rannik, Ü., Rebmann, C., Suyker, A., Valentini, R.,
694 Wilson, K., and Wofsy, S.: Seasonality of ecosystem respiration and gross primary production as
695 derived from FLUXNET measurements, Agricultural and Forest Meteorology, 113, 53-74,
696 [https://doi.org/10.1016/S0168-1923\(02\)00102-8](https://doi.org/10.1016/S0168-1923(02)00102-8), 2002.

697 Falge, E., Baldocchi, D., Olson, R., Anthoni, P., Aubinet, M., Bernhofer, C., Burba, G., Ceulemans, R.,

698 Clement, R., Dolman, H., Granier, A., Gross, P., Grünwald, T., Hollinger, D., Jensen, N.-O., Katul, G.,
699 Keronen, P., Kowalski, A., Lai, C. T., Law, B. E., Meyers, T., Moncrieff, J., Moors, E., Munger, J. W.,
700 Pilegaard, K., Rannik, Ü., Rebmann, C., Suyker, A., Tenhunen, J., Tu, K., Verma, S., Vesala, T., Wilson,
701 K., and Wofsy, S.: Gap filling strategies for defensible annual sums of net ecosystem exchange,
702 *Agricultural and Forest Meteorology*, 107, 43-69, [https://doi.org/10.1016/S0168-1923\(00\)00225-2](https://doi.org/10.1016/S0168-1923(00)00225-2),
703 2001.

704 Foken, T., Göckede, M., Mauder, M., Mahrt, L., Amiro, B., and Munger, W.: Post-Field Data Quality
705 Control, in: *Handbook of Micrometeorology: A Guide for Surface Flux Measurement and Analysis*,
706 edited by: Lee, X., Massman, W., and Law, B., Springer Netherlands, Dordrecht, 181-208,
707 [10.1007/1-4020-2265-4_9](https://doi.org/10.1007/1-4020-2265-4_9), 2005.

708 Hadden, D. and Grelle, A.: Net CO₂ emissions from a primary boreo-nemoral forest over a 10year
709 period, *Forest Ecology and Management*, 398, 164-173, <https://doi.org/10.1016/j.foreco.2017.05.008>,
710 2017.

711 Hayek, M. N., Longo, M., Wu, J., Smith, M. N., Restrepo-Coupe, N., Tapajos, R., da Silva, R.,
712 Fitzjarrald, D. R., Camargo, P. B., Hutrya, L. R., Alves, L. F., Daube, B., Munger, J. W., Wiedemann, K.
713 T., Saleska, S. R., and Wofsy, S. C.: Carbon exchange in an Amazon forest: from hours to years,
714 *Biogeosciences*, 15, 4833-4848, [10.5194/bg-15-4833-2018](https://doi.org/10.5194/bg-15-4833-2018), 2018.

715 Jia, X., Mu, Y., Zha, T., Wang, B., Qin, S., and Tian, Y.: Seasonal and interannual variations in
716 ecosystem respiration in relation to temperature, moisture, and productivity in a temperate semi-arid
717 shrubland, *Science of The Total Environment*, 709, 136210,
718 <https://doi.org/10.1016/j.scitotenv.2019.136210>, 2020.

719 KATO, T., TANG, Y., GU, S., HIROTA, M., DU, M., LI, Y., and ZHAO, X.: Temperature and biomass
720 influences on interannual changes in CO₂ exchange in an alpine meadow on the Qinghai-Tibetan
721 Plateau, *Global Change Biology*, 12, 1285-1298, <https://doi.org/10.1111/j.1365-2486.2006.01153.x>,
722 2006.

723 Kondo, M., Saitoh, T. M., Sato, H., and Ichii, K.: Comprehensive synthesis of spatial variability in
724 carbon flux across monsoon Asian forests, *Agricultural and Forest Meteorology*, 232, 623-634, 2017.

725 Konopka, J., Heusinger, J., and Weber, S.: Extensive Urban Green Roof Shows Consistent Annual Net
726 Uptake of Carbon as Documented by 5 Years of Eddy-Covariance Flux Measurements, *Journal of*

727 Geophysical Research: Biogeosciences, 126, e2020JG005879, 2021.

728 Krasnova, A., Mander, Ü., Noe, S. M., Uri, V., Krasnov, D., and Soosaar, K.: Hemiboreal forests' CO₂
729 fluxes response to the European 2018 heatwave, *Agricultural and Forest Meteorology*, 323, 109042,
730 <https://doi.org/10.1016/j.agrformet.2022.109042>, 2022.

731 Landsberg, J. and Waring, R.: A generalised model of forest productivity using simplified concepts of
732 radiation-use efficiency, carbon balance and partitioning, *Forest ecology and management*, 95, 209-228,
733 1997.

734 Laurin, G. V., Chen, Q., Lindsell, J. A., Coomes, D. A., Del Frate, F., Guerriero, L., Pirotti, F., and
735 Valentini, R.: Above ground biomass estimation in an African tropical forest with lidar and
736 hyperspectral data, *ISPRS Journal of Photogrammetry and Remote Sensing*, 89, 49-58, 2014.

737 Leuning, R. and King, K. M.: Comparison of eddy-covariance measurements of CO₂ fluxes by open-
738 and closed-path CO₂ analysers, *Boundary-Layer Meteorology*, 59, 297-311, [10.1007/BF00119818](https://doi.org/10.1007/BF00119818),
739 1992.

740 Li, L., Zhang, Y., Wu, J., Li, S., Zhang, B., Zu, J., Zhang, H., Ding, M., and Paudel, B.: Increasing
741 sensitivity of alpine grasslands to climate variability along an elevational gradient on the Qinghai-Tibet
742 Plateau, *Science of the Total Environment*, 678, 21-29, 2019.

743 Li, X. Y., Shi, F. Z., Ma, Y. J., Zhao, S. J., and Wei, J. Q.: Significant winter CO₂ uptake by saline lakes
744 on the Qinghai-Tibet Plateau, *Global Change Biology*, 28, 2041-2052, 2022.

745 Liu, C., Wu, Z., Hu, Z., Yin, N., Islam, A. T., and Wei, Z.: Characteristics and influencing factors of
746 carbon fluxes in winter wheat fields under elevated CO₂ concentration, *Environmental Pollution*, 307,
747 119480, 2022.

748 Liu, J., Zou, H.-X., Bachelot, B., Dong, T., Zhu, Z., Liao, Y., Plenković-Moraj, A., and Wu, Y.:
749 Predicting the responses of subalpine forest landscape dynamics to climate change on the eastern
750 Tibetan Plateau, *Global Change Biology*, 27, 4352-4366, <https://doi.org/10.1111/gcb.15727>, 2021.

751 Liu, N.-Y., Yang, Q.-Y., Wang, J.-H., Zhang, S.-B., Yang, Y.-J., and Huang, W.: Differential Effects of
752 Increasing Vapor Pressure Deficit on Photosynthesis at Steady State and Fluctuating Light, *Journal of*
753 *Plant Growth Regulation*, [10.1007/s00344-024-11268-0](https://doi.org/10.1007/s00344-024-11268-0), 2024.

754 Lloyd, J. and Taylor, J. A.: On the temperature dependence of soil respiration, *Functional Ecology*, 8,
755 315-323, 1994.

756 Mamkin, V., Avilov, V., Ivanov, D., Varlagin, A., and Kurbatova, J.: Interannual variability in the
757 ecosystem CO₂ fluxes at a paludified spruce forest and ombrotrophic bog in the southern taiga,
758 *Atmospheric Chemistry and Physics*, 23, 2273-2291, 10.5194/acp-23-2273-2023, 2023.

759 Mao, D., Luo, L., Wang, Z., Zhang, C., and Ren, C.: Variations in net primary productivity and its
760 relationships with warming climate in the permafrost zone of the Tibetan Plateau, *Journal of*
761 *Geographical Sciences*, 25, 967-977, 10.1007/s11442-015-1213-8, 2015.

762 Mauder, M. and Foken, T.: Documentation and Instruction Manual of the Eddy-Covariance Software
763 Package TK3 (update),

764 Mizoguchi, Y., Ohtani, Y., Takanashi, S., Iwata, H., Yasuda, Y., and Nakai, Y.: Seasonal and interannual
765 variation in net ecosystem production of an evergreen needleleaf forest in Japan, *Journal of Forest*
766 *Research*, 17, 283-295, 10.1007/s10310-011-0307-0, 2012.

767 Moncrieff, J. B., Massheder, J. M., de Bruin, H., Elbers, J., Friborg, T., Heusinkveld, B., Kabat, P.,
768 Scott, S., Soegaard, H., and Verhoef, A.: A system to measure surface fluxes of momentum, sensible
769 heat, water vapour and carbon dioxide, *Journal of Hydrology*, 188-189, 589-611,
770 [https://doi.org/10.1016/S0022-1694\(96\)03194-0](https://doi.org/10.1016/S0022-1694(96)03194-0), 1997.

771 Monson, R. K., Lipson, D. L., Burns, S. P., Turnipseed, A. A., Delany, A. C., Williams, M. W., and
772 Schmidt, S. K.: Winter forest soil respiration controlled by climate and microbial community
773 composition, *Nature*, 439, 711-714, 10.1038/nature04555, 2006.

774 Monteith, J. L., Unsworth, M. H., and Webb, A.: Principles of environmental physics, *Quarterly*
775 *Journal of the Royal Meteorological Society*, 120, 1699, 1994.

776 Mu, C., Mu, M., Wu, X., Jia, L., Fan, C., Peng, X., Ping, C. I., Wu, Q., Xiao, C., and Liu, J.: High
777 carbon emissions from thermokarst lakes and their determinants in the Tibet Plateau, *Global Change*
778 *Biology*, 2023.

779 Niu, Z., Jinniu, W., Xufeng, W., Dongliang, L., Cheng, S., and Aihong, G.: Net ecosystem CO₂ exchange
780 and its influencing factors in non-growing season at a sub-alpine forest in the core Three Parallel
781 Rivers region, *Acta Ecologica Sinica*, 43, 5967-5979, 10.5846/stxb202204020841, 2023.

782 World Meteorological Organization.: 2019 concludes a decade of exceptional global heat and
783 high-impactweather[EB/OL].[https://public.wmo.int/en/media/press-release/2019-concludes-decade-of-](https://public.wmo.int/en/media/press-release/2019-concludes-decade-of-exceptional-global-heat-and-high-impact-weather)
784 [exceptional-global-heat-and-high-impact-weather](https://public.wmo.int/en/media/press-release/2019-concludes-decade-of-exceptional-global-heat-and-high-impact-weather), 2019.

785 Pan, Y., Birdsey, R. A., Fang, J., Houghton, R., Kauppi, P. E., Kurz, W. A., Phillips, O. L., Shvidenko,
786 A., Lewis, S. L., and Canadell, J. G.: A large and persistent carbon sink in the world's forests, *Science*,
787 333, 988-993, 2011.

788 Pavelka, M., Acosta, M., Marek, M. V., Kutsch, W., and Janous, D.: Dependence of the Q10 values on
789 the depth of the soil temperature measuring point, *Plant and Soil*, 292, 171-179,
790 10.1007/s11104-007-9213-9, 2007.

791 Qu, S., Xu, R., Yu, J., and Borjigidai, A.: Extensive atmospheric methane consumption by alpine
792 forests on Tibetan Plateau, *Agricultural and Forest Meteorology*, 339, 109589,
793 <https://doi.org/10.1016/j.agrformet.2023.109589>, 2023.

794 Reichstein, M., Falge, E., Baldocchi, D., Papale, D., Aubinet, M., Berbigier, P., Bernhofer, C.,
795 Buchmann, N., Gilmanov, T., Granier, A., Grünwald, T., Havránková, K., Ilvesniemi, H., Janous, D.,
796 Knohl, A., Laurila, T., Lohila, A., Loustau, D., Matteucci, G., Meyers, T., Miglietta, F., Ourcival, J.-M.,
797 Pumpanen, J., Rambal, S., Rotenberg, E., Sanz, M., Tenhunen, J., Seufert, G., Vaccari, F., Vesala, T.,
798 Yakir, D., and Valentini, R.: On the separation of net ecosystem exchange into assimilation and
799 ecosystem respiration: review and improved algorithm, *Global Change Biology*, 11, 1424-1439,
800 <https://doi.org/10.1111/j.1365-2486.2005.001002.x>, 2005.

801 Schotanus, P., Nieuwstadt, F. T. M., and De Bruin, H. A. R.: Temperature measurement with a sonic
802 anemometer and its application to heat and moisture fluxes, *Boundary-Layer Meteorology*, 26, 81-93,
803 10.1007/BF00164332, 1983.

804 Schweizer, V. J., Ebi, K. L., van Vuuren, D. P., Jacoby, H. D., Riahi, K., Strefler, J., Takahashi, K., van
805 Ruijven, B. J., and Weyant, J. P.: Integrated Climate-Change Assessment Scenarios and Carbon
806 Dioxide Removal, *One Earth*, 3, 166-172, 10.1016/j.oneear.2020.08.001, 2020.

807 Schwinning, S. and Sala, O. E.: Hierarchy of responses to resource pulses in arid and semi-arid
808 ecosystems, *Oecologia*, 141, 211-220, 10.1007/s00442-004-1520-8, 2004.

809 Stein, T.: Carbon dioxide peaks near 420 parts per million at Mauna Loa observatory, NOAA Research,
810 June, 7, 2021.

811 Tang, X., Xiao, J., Ma, M., Yang, H., Li, X., Ding, Z., Yu, P., Zhang, Y., Wu, C., Huang, J., and
812 Thompson, J. R.: Satellite evidence for China's leading role in restoring vegetation productivity over
813 global karst ecosystems, *Forest Ecology and Management*, 507, 120000,

814 <https://doi.org/10.1016/j.foreco.2021.120000>, 2022.

815 Vote, C., Hall, A., and Charlton, P.: Carbon dioxide, water and energy fluxes of irrigated broad-acre
816 crops in an Australian semi-arid climate zone, *Environmental Earth Sciences*, 73, 449-465, 2015.

817 Wang, C.-Y., Wang, J.-N., Wang, X.-F., Luo, D.-L., Wei, Y.-Q., Cui, X., Wu, N., and Bagaria, P.:
818 Phenological Changes in Alpine Grasslands and Their Influencing Factors in Seasonally Frozen
819 Ground Regions Across the Three Parallel Rivers Region, Qinghai-Tibet Plateau, *Frontiers in Earth
820 Science*, 9, 10.3389/feart.2021.797928, 2022.

821 Wang, S., Grant, R., Verseghy, D., and Black, T.: Modelling plant carbon and nitrogen dynamics of a
822 boreal aspen forest in CLASS—the Canadian Land Surface Scheme, *Ecological Modelling*, 142,
823 135-154, 2001.

824 Wang, Y., Yao, G., Zuo, Y., and Wu, Q.: Implications of global carbon governance for corporate carbon
825 emissions reduction, *Frontiers in Environmental Science*, 11, 3, 2023a.

826 Wang, Y., Sun, Y., Chen, Y., Wu, C., Huang, C., Li, C., and Tang, X.: Non-linear correlations exist
827 between solar-induced chlorophyll fluorescence and canopy photosynthesis in a subtropical evergreen
828 forest in Southwest China, *Ecological Indicators*, 157, 111311,
829 <https://doi.org/10.1016/j.ecolind.2023.111311>, 2023b.

830 Wang, Y., Xiao, J., Ma, Y., Ding, J., Chen, X., Ding, Z., and Luo, Y.: Persistent and enhanced carbon
831 sequestration capacity of alpine grasslands on Earth's Third Pole, *Science Advances*, 9,
832 eade6875, doi:10.1126/sciadv.ade6875, 2023c.

833 Wang, Y., Xiao, J., Ma, Y., Luo, Y., Hu, Z., Li, F., Li, Y., Gu, L., Li, Z., and Yuan, L.: Carbon fluxes and
834 environmental controls across different alpine grassland types on the Tibetan Plateau, *Agricultural and
835 Forest Meteorology*, 311, 108694, 2021.

836 Wehr, R., Munger, J. W., McManus, J. B., Nelson, D. D., Zahniser, M. S., Davidson, E. A., Wofsy, S. C.,
837 and Saleska, S. R.: Seasonality of temperate forest photosynthesis and daytime respiration, *Nature*, 534,
838 680-683, 10.1038/nature17966, 2016.

839 Wu, T., Ma, W., Wu, X., Li, R., Qiao, Y., Li, X., Yue, G., Zhu, X., and Ni, J.: Weakening of carbon sink
840 on the Qinghai-Tibet Plateau, *Geoderma*, 412, 115707,
841 <https://doi.org/10.1016/j.geoderma.2022.115707>, 2022.

842 Y, W. Z., Y, L. Z., K, D. S., L, F. M., S, L. Y., M, L. S., N, W. S., H, M. C., X, M. T., and Y, C.:

843 Evolution of ecological patterns and its driving factors on Qinghai-Tibet Plateau over the past 40 years,
844 *Acta Ecologica Sinica*, 42, 8941-8952, 2022.

845 Yasin, A., Niu, B., Chen, Z., Hu, Y., Yang, X., Li, Y., Zhang, G., Li, F., and Hou, W.: Effect of warming
846 on the carbon flux of the alpine wetland on the Qinghai-Tibet Plateau, *Frontiers in Earth Science*, 10,
847 10.3389/feart.2022.935641, 2022.

848 YU, G. and SUN, X.: Principles of flux measurement in terrestrial ecosystem, Beijing: Higher
849 Education Press, 2006.

850 Yu, Y.: Double-order system construction of China's climate change legislation under the dual carbon
851 goals, *China Population Resources and Environment*, 32, 89-96, 2022.

852 Zemin, Z., Fenggui, L., Qiong, C., Xingsheng, X., and Qiang, Z.: Spatial Prediction of Potential
853 Property Loss by Geological Hazards based on Random Forest—A Case Study of Chamdo, Tibet,
854 *Plateau Science Research*, 7, 21-30, 10.16249/j.cnki.2096-4617.2023.02.003, 2023.

855 Zhang, J., Lin, H., Li, S., Yang, E., Ding, Y., Bai, Y., and Zhou, Y.: Accurate gas extraction (AGE)
856 under the dual-carbon background: Green low-carbon development pathway and prospect, *Journal of*
857 *Cleaner Production*, 134372, 2022.

858 Zhang, Y., Zhu, W., Sun, X., and Hu, Z.: Carbon dioxide flux characteristics in an *Abies fabri* mature
859 forest on Gongga Mountain, Sichuan, China, *Acta Ecologica Sinica*, 38, 6125-6135, 2018.